



FACULTAD DE CIENCIAS  
UNIVERSIDAD DE CANTABRIA

---

**Search for dark matter production in  
association with top quarks in the  
dilepton final state at  $\sqrt{s} = 13$  TeV**

---

A thesis submitted in fulfillment of the requirements for the  
**Degree of Doctor of Philosophy**

---

Written by

**Cédric Prieur**

Under the supervision of  
**Juan Piedra Gómez**  
**Pablo Martínez Ruiz del Río**

Santander, June 2020



# **Abstract**



# **Resumen**



# Acknowledgements



# Acronyms used

**SM** Standard Model

**DM** Dark Matter

**LHC** Large Hadron Collider

**CMS** Compact Muon Solenoid

**ATLAS** A Toroidal LHC Apparatus

**CERN** European Council for Nuclear Research

**CMB** Cosmic Microwave Background

**ML** Machine Learning

**MFV** Minimal Flavour Violation

**WIMP** Weakly Interactive Massive Particles

**PF** Particle Flow

**BSM** Beyond the Standard Model

**MACHO** Massive Compact Halo Objects

**SI** Spin Independant

**SD** Spin Dependant

**CL** Confidence Level

**QCD** Quantum ChromoDynamics

**ADMX** Axion Dark Matter Experiment

**CAST** CERN Axion Solar Telescope

**IAXO** International Axion Observatory

**UED** Universal Extra Dimensions

**NFW** Navarro-Frenk-White

**LAT** Fermi Large Telescope

**IACT** Imaging Atmospheric Cherenkov Telescopes

**CTA** Cherenkov Telescope Array

**AMS** Alpha Magnetic Spectrometer

**EFT** Effective Field Theory

**ISR** Initial State Radiation

**DMWG** Dark Matter Working Group

**MET** Missing Transverse Energy

**VBF** Vector Boson Fusion

# Contents

<b>1</b>	<b>Introduction</b>	<b>1</b>
<b>2</b>	<b>The Dark Matter case</b>	<b>5</b>
2.1	The Standard Model (SM) . . . . .	5
2.2	At the origins of dark matter . . . . .	5
2.2.1	Zwicky and the virial theorem . . . . .	6
2.2.2	Spiral galaxies rotation curves . . . . .	6
2.2.3	Cosmic Microwave Background (CMB) anisotropies . . . . .	7
2.2.4	Gravitational lensing . . . . .	9
2.3	Dark matter properties . . . . .	10
2.4	Dark matter candidates . . . . .	12
2.5	Dark matter searches . . . . .	18
2.5.1	Direct searches . . . . .	19
2.5.2	Indirect searches . . . . .	23
2.5.3	Collider production . . . . .	27
2.6	Dark Matter (DM) production at the Large Hadron Collider (LHC) . . . . .	30
2.6.1	The single top production channel . . . . .	33
2.6.2	The $t\bar{t}$ production channel . . . . .	33
2.6.3	The dilepton final state . . . . .	33
2.7	Previous relevant results . . . . .	33
<b>3</b>	<b>The experimental device</b>	<b>37</b>
3.1	The LHC accelerator . . . . .	37
3.2	The CMS detector . . . . .	37
3.2.1	Tracker . . . . .	37
3.2.2	Electromagnetic calorimeter . . . . .	37

3.2.3	Hadronic calorimeter . . . . .	37
3.2.4	Muon system . . . . .	37
3.2.5	Trigger . . . . .	37
3.2.6	Data acquisition . . . . .	37
<b>4</b>	<b>Objects reconstruction</b>	<b>39</b>
4.1	Particle Flow algorithm . . . . .	39
4.2	Leptons reconstruction . . . . .	39
4.2.1	Electrons . . . . .	39
4.2.2	Muons . . . . .	39
4.3	Jets reconstruction . . . . .	39
4.3.1	B-tagging . . . . .	39
4.4	Missing transverse energy . . . . .	39
4.5	Top reconstruction . . . . .	39
<b>5</b>	<b>Data, signals and backgrounds</b>	<b>41</b>
5.1	Data samples . . . . .	41
5.2	Signal samples . . . . .	41
5.3	Background prediction . . . . .	41
5.3.1	The main background: $t\bar{t}$ . . . . .	41
5.3.2	Drell-Yan estimation . . . . .	41
5.3.3	Non prompt contamination . . . . .	41
5.3.4	Smaller backgrounds . . . . .	41
5.3.5	Weights and corrections applied . . . . .	41
<b>6</b>	<b>Event selection</b>	<b>43</b>
6.1	Signal regions . . . . .	43
6.2	Control regions . . . . .	43
6.3	Background-signal discrimination . . . . .	43
6.3.1	Discriminating variables . . . . .	43
6.3.2	Neural network . . . . .	43
<b>7</b>	<b>Results and interpretations</b>	<b>45</b>
7.1	Systematics and uncertainties . . . . .	45

7.2 Results . . . . .	45
<b>8 Conclusions</b>	<b>47</b>
8.1 Future prospects . . . . .	47
<b>Appendices</b>	<b>49</b>
<b>Bibliography</b>	<b>55</b>

# Chapter 1

## Introduction

The SM of particle physics is nowadays the most accepted mathematical model used to describe the elementary particles and three of the four fundamental forces of nature (electromagnetic, weak and strong interactions). This model is quite simple in concept, but has been able to describe most of the phenomena observed in nature so far with an incredible level of precision, and made a lot of predictions that have now been proven to be true, such as the postulate of the Higgs mechanism [1, 2] followed by the discovery of the Higgs boson itself in 2012 [3, 4] by the Compact Muon Solenoid (CMS) and A Toroidal LHC ApparatuS (ATLAS) experiments of the European Council for Nuclear Research (CERN).

However, as accurate as it seems to be, this theory is known to have several shortcomings which require further investigation. Eventual exotic particles which do not fit in the current model could be the sign of new physics and have therefore been extensively searched for over the course of the last decades in order to enhance our understanding of the Universe and all its constituents.

In this context, the first serious DM hypothesis was introduced in the 1970s because of gravitational anomalies observed by several astrophysicists, as a way to explain the apparent non-luminous missing mass in the Universe [5]. Indeed, the visible mass in most galaxies appears to be way too low to explain several astrophysical processes, such as the rotation curves of the galaxies [6], which seems to be incompatible with the well established laws of gravitation. Some additional measurements of the gravitational lensing (in the Bullet Cluster, for example [7]) and the anisotropies observed in the CMB [8] can be quoted among other evidences for the existence of DM, as explained in details in Section 2.2.

As far as we currently know from cosmological measurements, ordinary baryonic matter only constitutes around 5% of the Universe, while DM represents around 26% of the energy density of the Universe (the rest is being considered as dark energy) [9]. Understanding the nature and properties of this new kind of exotic matter is therefore crucial to try and understand the physics in the Universe.

Nowadays, the existence of DM is well established in the physics community, even though it has never been observed directly, since our only evidences so far for its existence come from its large-

scale gravitational effects. While its mass, spin, nature and basic properties are still unknown and extensively studied, one of the best DM candidate is the so-called Weakly Interactive Massive Particles (WIMP), predicted to interact both gravitationnaly and weakly with SM particles. This would allow direct and indirect direction of such candidates, used as the driving process of many of experiments over the last decades, trying to find the hint of a possible interaction between standard baryonic particles and eventual DM particles, or even between several DM particles themselves. Dark matter production through the use of a particle accelerator colliding SM particles together, such as the LHC, is also a possibility, and will be consider as the main channel towards the eventual detection of this exotic matter throughout this work. The production through colliders is actually able to provide constraints on low dark matter masses as well, in a region where both the direct and indirect searches are less efficient, which makes the LHC a perfect tool to study this kind of Beyond the Standard Model (BSM) physics.

However, observing DM is still extremely difficult, mainly because it barely interacts with ordinary baryonic matter, except through gravity (we have to assume that it does interact with SM at least weakly for the sake of this work though, as we would not be able to discover it as an individual particle if it were not the case). This means that nowadays, all the experiments searching for DM have only been able to put constraints on the DM particle mass and on the interaction cross sections between the dark and standard sectors. Actually, even if the collisions between protons produced by the LHC do have an sufficient amount of energy to produce this kind of particles, we would not expect them to interact with our detector, meaning that a direct detection is out of our hands for now. The eventual presence of such matter has to be inferred from the study of the interaction between SM particles and CMS itself, since a typical DM-like event consists of at least one energetic SM particle produced in association with a large imbalance in the transverse momentum due to the presence of an eventual DM candidate that was able to escape our detection.

In the context of this work, DM is searched for in association with one or two top quarks which play the role of the SM particle allowing us to trigger the event. This is indeed a perfect channel for this kind of searches if we assume that the interaction between the dark and standard sectors respect the principle of Minimal Flavour Violation (MFV), which can be consistently defined independently of the structure of the new physics model [10]. In this case, this interaction should follow the same Higgs-like Yukawa coupling structure as the usual SM baryonic particles. This is an important consequence, since it will be shown in Section 2.3 that this coupling is actually stronger with more massive particles: the heavier the SM particle considered is, the easier it is for this particle to couple with the dark sector. This makes the top quark, the most massive of all the fundamental particles observed by far, is therefore an excellent object to study in this context.

However, this also means that its phenomenology is mostly driven by its large mass and that it decays before hadronization can occur, usually into a W boson and and a bottom quark ( $\sim 96\%$  branching ratio [11]). The final state of the process we are interested in is then be made of some b jets, leptons and/or quarks and is be categorized depending on this number of b jets and on the decay of the W itself. This work will actually be focused on the two leptons final state, also known as the dileptonic channel, mostly since this channel does not have lots of background processes

raising to a similar final state, even though its branching ratio is the smallest, as will be explained in Section 2.6. Additionally, leptons are by reconstruction much cleaner than jets. This means that their identification and momentum calculation is easier to perform, and that the uncertainties associated to these measurements will be smaller.

The LHC has now been running for 10 years, and several similar searches have already been carried out and published in the past by the CMS and ATLAS collaborations, at different center of mass energies. First of all, at 8 TeV, several searches for a pair of top quarks were published by the CMS (in association with DM in the semileptonic [12] and dileptonic [13] final states) and ATLAS collaborations [14]. At 13 TeV, the ATLAS collaboration published on one hand several studies, considering different final states and different luminosities ( $13.3 \text{ fb}^{-1}$  and  $36.1 \text{ fb}^{-1}$ ) [15, 16, 17].

On the other hand, the CMS collaboration published a few extremely important papers for this study [19, 20]. For the first time in 2019, the results obtained by the  $t/\bar{t}+\text{DM}$  and  $t\bar{t}+\text{DM}$  analyses have also been combined and published using the 2016 data [21]. Our main objective is now to repeat and improve this analysis that was performed while considering a larger dataset, globally improving the analysis strategy and including the dileptonic final state for the first time in this combination.

After a general introduction about DM in general, the experimental device will be detailed in the Chapter 3. This will include a discussion about the LHC itself, along with a complete description of CMS, the detector used to collect the data that will be analyzed throughout this work. This data has been collected during the years 2016, 2017 and 2018 and corresponds to an integrated luminosity of  $\sim 138 \text{ fb}^{-1}$ , collected during the Run II of operation of the LHC and at a center of mass energy  $\sqrt{s} = 13 \text{ TeV}$ . In particular, a particular care will be given to the explanation of the Particle Flow (PF) algorithm, used to reconstruct the different objects used and that will be defined in the Chapter 4, while the estimation of the different backgrounds and the selection of interesting events will be detailed throughout the Chapters 5 and 6.

Distinguishing between the signal we are searching for and backgrounds having a much higher cross-section and kinematically really close, such as the SM  $t\bar{t}$  without production of DM is not a straightforward task (sometimes a production of missing transverse energy due to the presence of physical neutrinos is even obtained). To isolate the signal and to obtain some discrimination between these kind of processes, an algebraic reconstruction of the event and top-notch Machine Learning (ML) techniques are used in this work, in order to train a network of neurons. The main objective is to make them learn how to combine the discriminating power of a set of input variables in order to create a single output variable describing the probability of a single event to be classified as signal or background. All this process will be detailed in Section 6.3.

Finally, a statistical interpretation of our data will be performed and different sources of systematic uncertainties will be considered in the Chapter 7. This will allow us to set upper limits on the cross section production value of DM particles in our particular channel and for the simplified models considered in this analysis. The conclusions of this work and some additional future prospects will then finally be presented in Chapter 8.



# Chapter 2

## The Dark Matter case

In this chapter, some general explanations about Standard Model (SM) will first of all be given in Section 2.1 as a general introduction about today's most accepted mathematical model describing all the known particles and their interactions. The case for Dark Matter (DM) will then be presented in Section 2.2, along with a summary of the main evidences, mostly astrophysical, which lead to the introduction of this kind of Beyond the Standard Model (BSM) physics. Then, the main properties expected by such exotic matter will be introduced in Section 2.3 and nowadays's most accepted DM candidates, such as the Weakly Interactive Massive Particles (WIMP) briefly introduced previously will be presented in Section 2.4.

The main ways we have to search for this new exotic physics will then be shown in Section 2.5. Finally, the searches performed in colliders such as the Large Hadron Collider (LHC) and our particular channels of interest (DM produced in association with either one or two top quarks) will be detailed in Section 2.6 and the latest similar results and exclusion plots published over the course of the previous years by the ATLAS and CMS collaborations will be shown in Section 2.7.

### 2.1 The Standard Model (SM)

### 2.2 At the origins of dark matter

The origin of the concept of dark matter can be traced back to the 17 and 18th centuries, shortly after Newton's works on gravitation, even though this concept changed a lot over the years. Back then, DM was more considered to be ordinary matter which simply did not emit any kind of electromagnetic radiation, being therefore invisible and dark, but which does have a strong impact in the gravitational point of view because of its mass. It was for example considered in the 20th century to be found in massive astronomical objects able to absorb the light or other objects located behind them, such as black holes.

### 2.2.1 Zwicky and the virial theorem

Around this time, the first experimental evidences for the existence of dark matter were shown. In 1933, Fritz Zwicky managed to determine the mass of the Coma Cluster using the virial theorem [22], which states that if in a cluster in equilibrium under its own gravitation, the kinetic energy must be comparable to the gravitational binding energy.

Mathematically, the virial theorem can be written in Equation 2.1, where the brackets represents the mean value of the quantity obtained over time or position, the universal constants of gravitation  $G = 6.67 \cdot 10^{-11} \text{ m}^3 \text{ kg}^{-1} \text{ s}^{-2}$  and where the gravitation potential energy expression can be simplified assuming a spherical distribution of the masses and the same average density everywhere in the cluster.

$$2\langle T \rangle + \langle V \rangle = 0, \text{ where } \begin{cases} T = \frac{1}{2} \sum_i M_i v_i^2 = \frac{1}{2} M \langle v^2 \rangle \\ V = -4\pi G \int_0^R M \rho r dr \propto \frac{GM^2}{R} \end{cases} \quad (2.1)$$

Solving these simple equations gives us an approximate value of the mass of the cluster in Equation 2.2, where  $R$  is the radius of the cluster and  $\langle v^2 \rangle$  is the squared velocity of all the galaxies averaged over time.

$$M \propto \frac{\langle \langle v^2 \rangle \rangle R}{G} \quad (2.2)$$

From this simple expression and astronomical observations, Zwicky then managed to compute the average mass to light ratio of its galaxies and concluded that the value obtained was around 500 times larger than the mass previously estimated by Edwin Hubble, who simply considered the number of visible galaxies within this cluster. One plausible explanation for this discrepancy is to introduce the concept dark matter, which contributes to the mass of the cluster without increasing the galactic luminosity.

Zwicky's results were actually quite controversial since they were based on statistical calculations relying on different hypotheses not always justified, such as the fact that the galaxies in the cluster must be gravitationnaly bound with each other and they were actually proven to be overestimated later on [23].

### 2.2.2 Spiral galaxies rotation curves

Despite being controversial and slightly off, Zwicky's results were soon followed by a series of additional astronomical observations leading to the same conclusion, the possible existence of non-luminous matter in all the galaxies, called dark matter. The most famous of these results is the

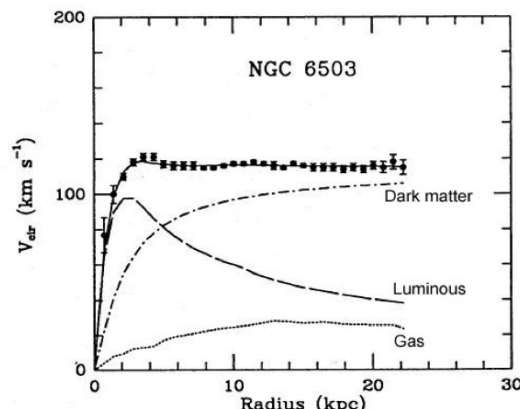
study of the observed and expected rotation curves of the stars within spiral galaxies such as the Milky Way in the 1970s [6].

According to this study, if we assume that we can apply Newton's universal laws of gravitation at the galactic scale, then the stars within this kind of galaxies should rotate with a velocity depending on the radius to the galactic center obtained by the usual equation for centripetal acceleration in a gravitational field and represented in Equation 2.3, where  $M(r)$  accounts for the total mass encountered in a radius  $r$ .

$$v_{\text{rotation}}(r) = \sqrt{\frac{GM(r)}{r}} \quad (2.3)$$

At first approximation, one can assume that most of the mass within this kind of galaxies comes from the inner core, meaning that, at large radius, the velocity of individual stars is expected to decrease proportionally to  $r^{-1/2}$ . Any deviation to this rule suggest that either our understanding of gravity at large scales has to be revised, or that our basic understanding of galaxies as a celestial body made of stars, dust and gas, has to be revised.

However, observations made by Vera Rubin and her team in the early 1970s with a new spectrograph designed the velocity curves of spiral galaxies with a degree of accuracy never reached before, did not confirm these expectations [24]. Indeed, according to these results, from a given value of the radius, the velocity curve appears to be flat instead of decreasing as expected, as illustrated in Figure 2.1.



K.G. Begeman, A.H. Broeels, R.H. Sanders. 1991. Mon.Not.RAS 249, 523.

Figure 2.1: Expected and observed rotation curves of the galaxy NGC 6503 [6]. The black dots correspond to the data and the *luminous* line corresponds to the expected rotation curve.

### 2.2.3 Cosmic Microwave Background (CMB) anisotropies

The CMB is a mostly uniform background of primary radio waves emitted when the Universe became transparent around 380.000 years after the Big Bang and was discovered accidentally in the 1940s [25]. Studying it is extremely important, as it is actually made of the oldest and cleanest electromagnetic

radiation we can find in the Universe. Precise measurements of this radiation are actually critical in many different fields of physics, since any proposed model of the Universe must be able to explain this radiation, its temperature and anisotropies.

Recent measurements determined that the CMB can be considered as emitting a thermal black body spectrum at a temperature of  $(2.72548 \pm 0.00057)\text{K}$  [26]. However, we now know that this temperature is actually not constant as some small anisotropies (at the  $10^{-5}$  level) depending on the value of the angular angle of observation can be observed, as represented on Figure 2.2.

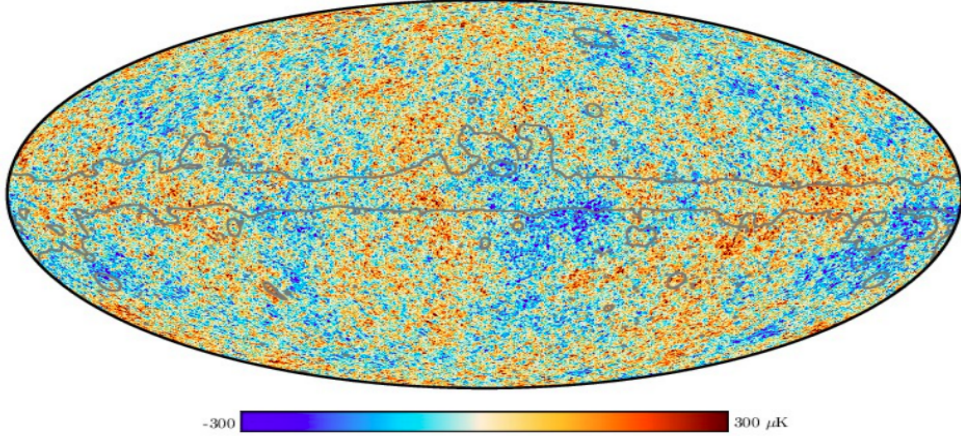


Figure 2.2: Anisotropies in the temperature of the CMB, as observed by the Planck satellite in 2018 [27].

We see these fluctuations projected over a 2D sphere, and it is therefore natural to introduce at this point Laplace's spherical harmonics,  $Y_{lm}(\theta, \phi)$ , a complete set of orthogonal functions defined on a sphere and defined by a few parameters such as  $l$ , the multipole, representing a given angular angle in the sky ( $l=100$  corresponds to  $\sim 1^\circ$ ) and  $m$ , the number of poles, such as  $-l \leq m \leq l$  [28].

The temperature fluctuations, whose value depend on the two usual spherical angles  $\theta$  and  $\phi$  can then be expanded using these generic functions, according to Equation 2.4.

$$\frac{\Delta T}{T}(\theta, \phi) = \sum_{l,m} a_{lm} Y_{lm}(\theta, \phi) \quad (2.4)$$

The information about the anisotropies can actually be extracted from the values of the  $a_{lm}$  coefficients, from which we can obtain the values needed to represent the power spectrum of the CMB, according to Equation 2.5, and from which most of the cosmological information of the CMB can actually be derived.

$$D_l = \frac{l(l-1)C_l}{2\pi} = \sum_m |a_{lm}^2| \quad (2.5)$$

Interestingly enough, this spectrum is directly affected by the value of the density of the dark

matter in the Universe. Doing a multi-parameters fit on the observed data in this plot is then able to give us directly the energy density of baryonic  $\Omega_b$  and dark  $\Omega_\chi$  matter, along with other important parameters of the  $\Lambda CDM$  cosmological model. Today's most precise measurements have been obtained in 2018 using the Plank satellite, and lead to the determination of these two quantities:  $\Omega_b h^2 = 0.02220 \pm 0.00020$  and  $\Omega_\chi h^2 = 0.1185 \pm 0.0015$  [29] and the actual power spectrum obtained represented in Figure 2.3.

By dividing these results with the value of the scaling factor for Hubble expansion rate  $h = 0.674$  [30], we can obtain from these numbers a proportion of 4.9% of ordinary baryonic matter and 26.1% of dark matter in the Universe.

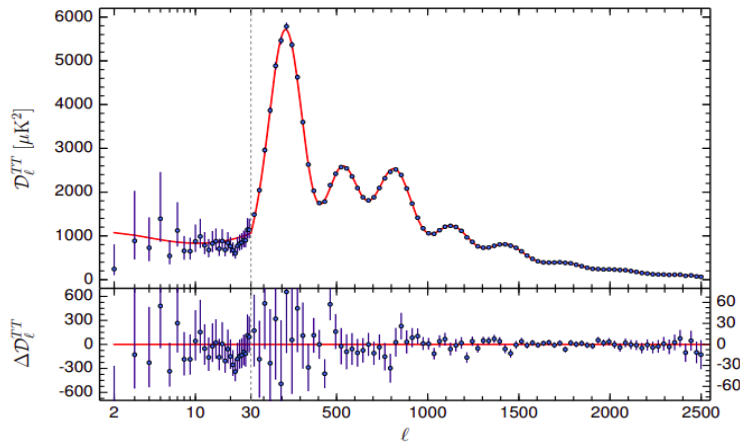


Figure 2.3: Power spectrum of the CMB obtained by Planck, representing the fluctuations of the temperature of this radiation with respect to the angular angle of observation.

## 2.2.4 Gravitational lensing

The last evidence supporting the existence of dark matter has been obtained by observing several clusters of galaxies in the Universe, such as the Bullet Cluster, and by studying their mass distribution through gravitational lensing. This effect is a consequence of the general relativity, a theory developed by Einstein has a way to represent gravity using the geometry of spacetime, stating that massive objects lying between distant sources and an observer should act as a lens and bend the light of the object emitted by the source. This deviation of the light is actually proportional to the mass of the object in between the source and the observer, meaning that the gravitational lensing can give us a way to measure the mass distribution within massive objects, such as galaxy clusters.

The bullet Cluster is particularly interesting in this context since it actually provides an evidence for the eventual existence of dark matter which does not rely on any mathematical assumption and cannot at principle be explained by alternate laws of gravitation. Indeed, some observations showed that the spatial deviations between the center of the total mass and the center of the baryonic mass cannot be explained with an alteration of the gravitational force law alone, with a statistical significance of  $8\sigma$  [31].

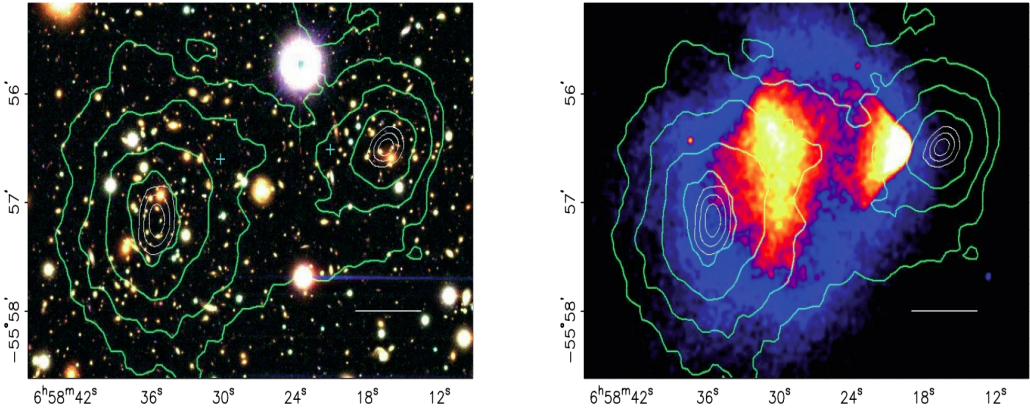


Figure 2.4: Mass distributions obtained by the Magellan in the visible (on the left) and Chandra on the X-rays spectrum (on the right) telescopes of the Bullet Cluser, yet another clear evidence for the existence of DM [31].

As seen in Figure 2.4, the image taken by Chandra clearly shows an offset between the plasma of the cluster and the actual mass distribution measured through gravitational lensing (green contours). The mass distribution appears to be slightly deviated compared to what was expected based on the X-ray emissions of this cluster.

## 2.3 Dark matter properties

All the previous observations allow us to list some of the most important properties that the perfect dark matter candidate should have. Even though several theories exist, each giving different properties to the DM, we will consider in this work the following mostly accepted properties for such particles:

- First of all, we will assume that DM is a **particle**. As far as we know, the Universe, is simply composed of particles so there is no objective reason to think that DM, being matter with a certain mass, might not be made of some kind of indivisible particle at some level.
- First of all, the perfect DM candidate should of course be **dark**. This means that it should not interact at all in with electromagnetic radiation such as light, and that it should therefore be **electrically neutral**. However, it has to interact gravitationnaly because of the evidences for the evidence of such a particle explained before, mostly relying on gravitational effects.
- It has to be **non-baryonic**, mainly because the energy density for the baryonic matter obtained by observing the power spectrum of the CMB is too low to account for DM as well, as explained in Section 2.2.3. Indeed, according to these results, baryonic matter account for around 5% while dark matter accounts for more than 25% of the energy density of the Universe.
- We will also only consider **cold** dark matter, since the widely accepted  $\Lambda$ *CDM* cosmological

model is actually based on this assumption. By cold, we do not refer to the temperature of these particles but actually to their size, and therefore to the velocity by which they can travel in the Universe. Large scale structures of the Universe such as we can observe them today cannot actually not be explained if DM is made of hot/relativistic particles, as represented in Figure 2.5.

- It is interesting to report as well that DM particles are expected to be found near the electroweak symmetry breaking scale, between **10 GeV and 1 TeV**. This is a consequence of the expected production mechanism of such particles, the so-called thermal freeze-out.

This principle tells us that at some point in the history, DM was in thermal equilibrium with other primordial SM particles, meaning that its production and annihilation rates were equal, as shown in Equation 2.6.

$$\chi\bar{\chi} \leftrightarrow e^+e^-, \mu^+\mu^-, q\bar{q}, W^+W^-, ZZ \quad (2.6)$$

However, because of the expansion of the Universe, at some point DM particles were simply too far apart from each other and these reactions maintaining this equilibrium became not efficient enough to maintain this equilibrium. At this stage, the abundance of DM became fixed: this is the freeze-out, as represented in Figure 2.3.

This principle is interesting because, as a rule of thumb, we can say that if a particle interacts heavily, it will stay longer in equilibrium and its freeze-out abundance will be smaller, so there is a mathematical relation between the strength of the SM/DM interaction  $g$ , the mass of the DM particle  $m_\chi$  and its actual abundance  $\Omega_\chi$  that can be measured, as expressed in Equation 2.7 [32].

$$\Omega_\chi \propto \frac{m_\chi^2}{g^4} \quad (2.7)$$

By using a typical value for  $g$  of the order of the Fermi coupling constant  $G_0^F \simeq 4.54 \cdot 10^{14} \text{ J}^{-2}$ , we can see that, in order to observe a freeze-out abundance comparable to the current one, the DM candidate should indeed have a mass between 10 GeV and 1 TeV.

In any case, DM is not expected to have a mass lower than 300 eV since at this scale, the phase space density that would be needed to explain this relic abundance of DM would simply violate the Pauli-exclusion principle [35].

- Finally, they should be **long-lived**. Indeed, we expect that DM particles were produced 13.8 billion years ago during the Big Bang, but it seems that we still see them today. They should then be stable particles, or their lifetime should at least be larger than the age of the Universe itself.

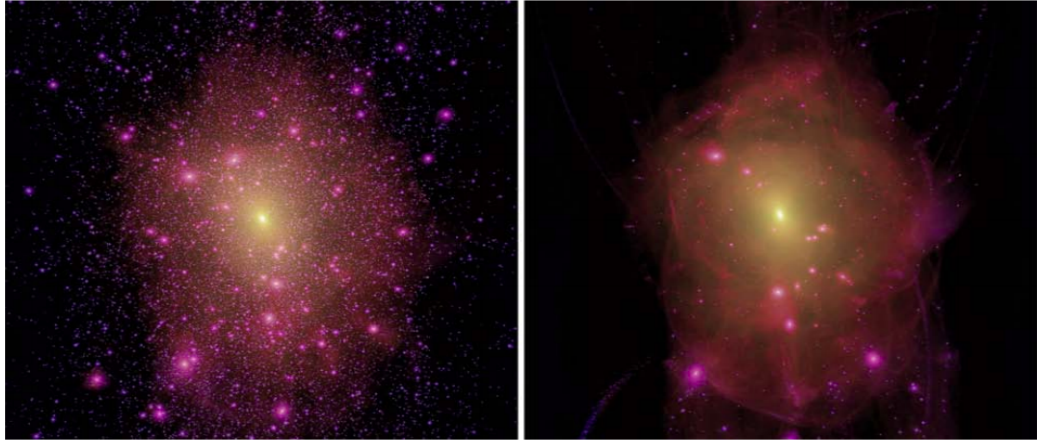
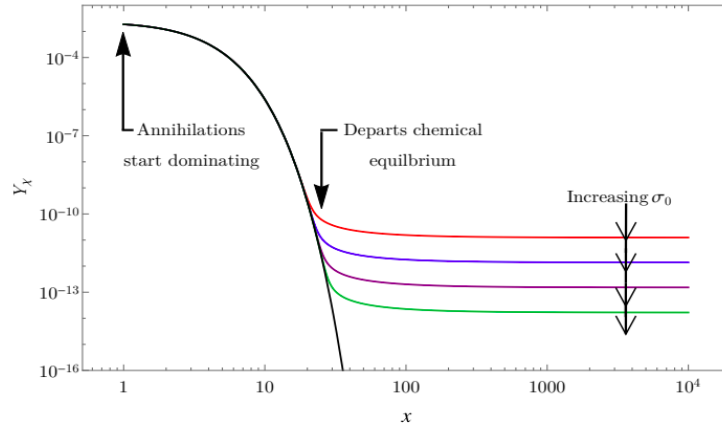


Figure 2.5: Computer simulations for cold (on the left) and warm (on the right) DM scenarios and their impact on a galactic halo at 0 redshift [33].



All these properties narrow quite a lot the number of possible DM candidates, as we will see in the following section.

## 2.4 Dark matter candidates

Several different categories of particles could pretend to be good candidates for dark matter. However, only the most interesting ones will be quoted here, since an extensive list of all the different possible candidates is out of the scope of this work. Two SM particles will first of all be investigating, before introducing some BSM theories giving us additional DM candidates with the right properties.

## Massive Compact Halo Objects (MACHO)

The first obvious DM candidate are the so-called MACHO. These objects are massive astronomical non-luminous bodies (such as black holes) made of baryonic matter and very hard to detect, that could be responsible of the gravitational lensing observed and that could explain the apparent missing mass in the Universe. However, as we saw in Section 2.3, DM is not expected to be made of such ordinary matter, mainly because observational data of the CMB and the deduced baryonic density of energy in the Universe is able to rule out this possibility.

Several different experiments did try to search for such DM anyway, and managed to constrain the properties of this kind of objects. The main way to search for such massive objects is through their gravitational lensing effect (actually, we talk about microlensing in this case since this effect is tiny) since, according to the general relativity, they should bend the light of luminous objects, such as stars, located behind them, and this bending actually depends on the mass of the eventual MACHO. Experiments like the MACHO project [36] and EROS [37] observed in this context  $\Theta(10^7)$  stars for several years, looking for microlensing events in order to constrain this particular DM model. Results published in 2000 from the MACHO project, after studying almost 12 million stars actually observed between 13 and 17 such events, way lower than expected if DM was only made out of MACHOs. The collaboration actually managed to exclude at the 95% Confidence Level (CL) the possibility of the dark halo to be entirely made of such baryonic particles [36]. On the other hand, the EROS collaboration only observed 1 microlensing after observing more than 30 millions of bright stars during 6.7 years, while  $\sim 39$  events were expected [37]. Both results have also been combined in order to obtain the exclusion plot represented in Figure 2.6. From this study, MACHO objects with low masses ( $10^{-7} M_\odot < m < 10^{-3} M_\odot$ ) make up less than 25% of the dark matter halo for most models considered at the 95% CL [38].

## Active neutrinos

SM *active* neutrinos  $\nu$  (as opposed to *sterile* neutrinos, that will be the subject of the discussion in the next section) have been considered as good DM candidates for a long time as well, since they are the only electrically neutral and long-lived SM particles, two important properties of any DM candidate. They have a few particular properties that might be interesting in this context.

- First of all, even though it has still not been measured precisely, their mass has been measured to be lower than 0.17 eV at the 95% CL from cosmological studies [42]. This is incredibly low compared to other SM particles, this particularity usually being referred to as the *mass puzzle* of the neutrinos.
- Their low mass means that the gravitational interaction between two neutrinos is usually considered to be null and that we can consider that they only interact weakly, making it hard to study their properties. Their actual cross-section, represented in Figure 2.7 and which of course depends on their energies and on the channel of interaction (neutral or charged current

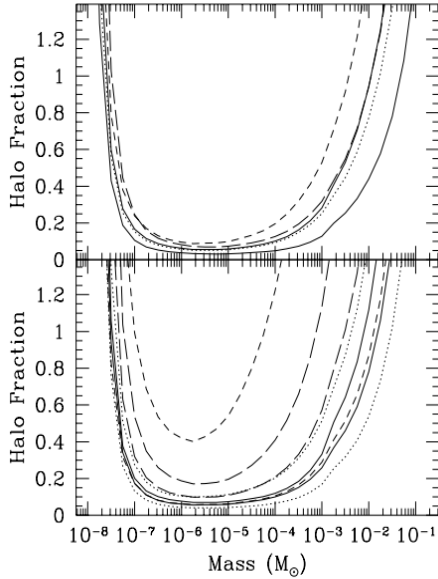


Figure 2.6: Halo fraction upper limit at the 95% CL compared to the mass of the lensing object for different MACHO models considered by the EROS (on the top) and the MACHO (on the bottom) collaborations [38].

considered).

This figure clearly shows that an approximate value of the cross section for such neutrinos is of the order of magnitude of  $10^{-38} \text{ cm}^2 \text{ GeV}^{-1}$ , which is typically tens of orders of magnitude lower than the interaction cross section of a photon ( $\sigma_\gamma \sim 10^{-25} \text{ cm}^2$  [40]). This means that the typical neutrinos of a few MeV produced by nuclear reactors have a mean free path of approximately 10 light years in steel.

- Neutrinos are also the only SM particle only observed in their left-handed chirality state, while anti-neutrinos can only be observed in their right-hand state. This could mean two things: either right-handed do not exist in nature for some reason, or we have just not been able to detect them because their interaction with baryonic matter is too weak. Right-handed neutrinos, also referred to as *sterile* neutrinos do not fit in the current SM but could anyway also be a strong BSM DM candidate, as we will discuss in the next subsection.
- Finally, neutrinos can oscillate, a quantum phenomena according to which the flavor of a neutrino can spontaneously change with time. This means that the three interacting states  $\nu_\alpha$  that we can observe are actually composed of several mass eigenstates  $\nu_i$ , as related in Equation 2.8, where these states can be related using the so-called Pontecorvo-Maki-Nakagawa-Sakata matrix  $(V_\nu)_{\alpha i}$ .

$$\nu_\alpha = (V_\nu)_{\alpha i} \nu_i \quad (2.8)$$

This effect does not however at principle have anything to do with the fact that they can be considered DM candidates, so this subject will not be discussed further in this work.

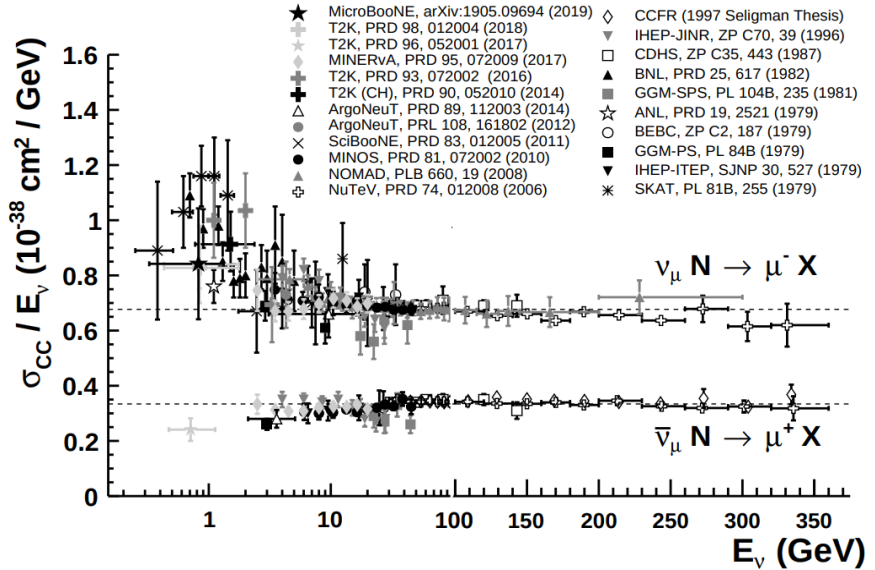


Figure 2.7: Neutrino cross section from the charged current as measured by different experiments over a large range of energies, for both neutrinos  $\nu$  and antineutrinos  $\bar{\nu}$  [39].

However, two physical reasons can explain why we do not really believe that DM could be made of neutrinos any more. First of all, their relative abundance does not match the expected one for DM from the freeze-out mechanism explained in Section 2.3. Indeed, their freeze-out abundance can be computed quite easily from Equation 2.9 [41], where the sum of the masses of the three neutrino flavors has been calculated to be lower than 0.17 eV [42] instead of 11.5 eV expected to obtain the correct DM abundance as observed today from the power spectrum of the CMB.

$$\Omega_\nu h^2 = \sum_{i=1}^3 \frac{m_{\nu_i}}{93 \text{ eV}} \quad (2.9)$$

Additionally, for several reasons explained in Section 2.3, a good DM candidate is expected to be cold, i.e. non-relativistic. However, being extremely light, neutrinos are expected to be ultra-relativistic and could therefore not be responsible of the emergence of large scale structures as observed today. We can therefore most probably rule out the possibility of DM being made of SM neutrinos.

### Sterile neutrinos

The most obvious SM particles being ruled out as DM candidates, it is now time to introduce some of the most famous BSM theories introducing additional particles that could have the properties searched for. The first one of these theories introduce the so-called sterile neutrinos, usually referring to the right-handed SM neutrinos, as discussed in the previous subsection.

If they exist, sterile neutrinos are expected in a much weaker way than SM neutrinos, they could

be very long-lived as well and at principle, nothing prevents us from considering that they could have a mass superior to 0.4 keV, giving therefore the correct DM relic abundance [35]. A superior bound of 50 keV on such particles can also be obtained considering limits on the observation of the monochromatic decay line originating from the one loop radiative decay  $N \rightarrow \nu + \gamma$  of such particles.

Several experiments are already searching for such particles at this level of energy. Most of these experiments focus on the analysis of  $\gamma$ -rays and are actually searching this monochromatic line resulting of the decay of sterile neutrinos. Two independant groups actually announced in 2014 the observation of an unidentified emission line at 3.57 keV (Figure 2.8) which does not match any known atomic emission line and which is actually consistent with an eventual DM signal [43, 44], since most of the possible instrumental contamination effects have now been ruled out.

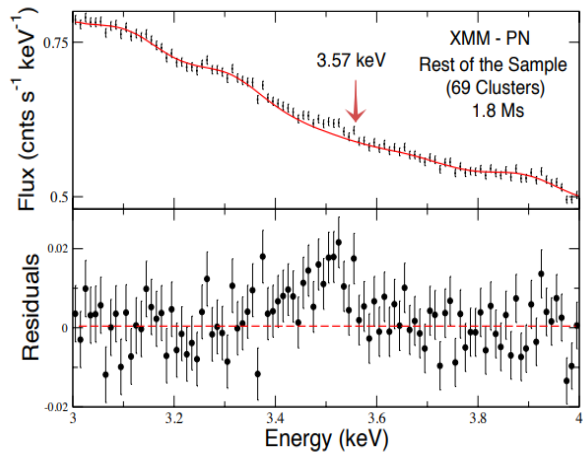


Figure 2.8: 3.57 keV emission line detected with a  $4.5\sigma$  CL by the XMM-Newton telescope in 2014, which could be a hint of the presence of DM [43].

However, studies of the galactic center pointed out the fact that this observation might actually come from the observation of a potassium K XVIII transition line [45]. Recent observations actually ruled out at the 99% CL an eventual DM origin for this particular line [46], but further studies are still ongoing.

## Axions

Axions could also explain the particle nature of DM, since its existence could explain 100% of the DM in the Universe, unlike the other candidates presented so far. Axions are hypothetical stable neutral particles, with masses of the order of the meV, introduced as a consequence of the solution of the CP violation issue of Quantum ChromoDynamics (QCD). This issue is the following: in the usual  $\Theta$  term of the QCD Lagrangian shown in Equation 2.10 [47] should be responsible of breaking the CP symmetry, but this effect has never been observed so far. This is the so-called the strong CP problem. Two ways to explain that we never observed this phenomena exist: the first is to assume that one of the quarks of the SM is massless but does not match the current observations, and the second is to assume that the parameter  $\Theta$ , the QCD vacuum angle, is small enough, so that this

term becomes negligible. However, by definition, the  $\Theta$  angle should be between 0 and  $2\pi$ , so there is no physical reason for this parameter to be small, unless some new physics, as the one developed in 1977 by Peccei and Quinn [48] by relaxing  $\Theta$  from a parameter to a dynamic variable and absorbing it through the introduction of a new pseudoscalar particle called the axion.

$$\mathcal{L}_\Theta = \frac{\Theta}{32\pi^2} \epsilon_{\mu\nu\rho\sigma} G_a^{\mu\mu} G_a^{\rho\sigma} \quad (2.10)$$

By definition, it is possible to show that axions satisfy two of the previous criteria for a good DM candidate, since they are non-relativistic and their abundance might be enough to account for the dark matter energy density observed, since their actual abundance can be obtained by Equation 2.11 [49], from which we could conclude that an axion having a mass of  $\sim 20$   $\mu\text{eV}$  could account for the actual dark matter density of the Universe, as observed today.

$$\Omega_a \simeq \left( \frac{6\mu\text{eV}}{m_a} \right)^{7/6} \quad (2.11)$$

Several axions searches experiments have therefore been set up, such as the Axion Dark Matter Experiment (ADMX), a resonant microwave cavity installed at the University of Washington, CERN Axion Solar Telescope (CAST), a CERN experiment observing the Sun which came online in 2002 and which managed in 2014 to turned up definitely the existence of solar axions [50], or the International Axion Observatory (IAXO), whose aim would be to search for axions with a much better signal to ratio noise than CAST. All the results obtained by these experiments along with their future projections are represented in Figure 2.12.

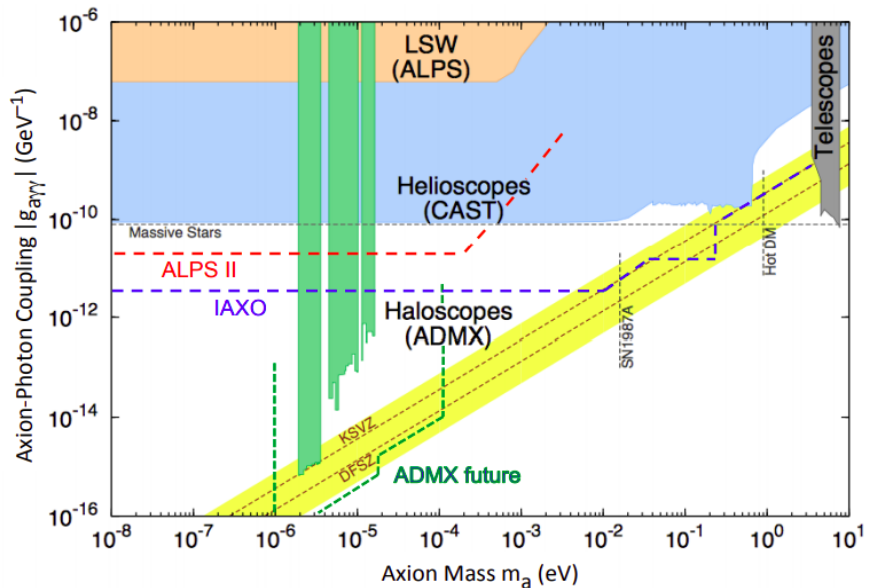


Figure 2.9: Axion exclusion plot summary and projected coverage of actual experiments [49].

## Weakly Interactive Massive Particles (WIMP)

The actual DM candidate that will be mostly considered throughout this work are the so-called Weakly Interactive Massive Particles (WIMP), which are expected to interact, even though very weakly, with ordinary baryonic matter and which have an expected mass in the range of 100 GeV to 1 TeV for reasonable electroweak production cross-section values, right where we expect DM to be found from its relic density: this is the so-called "WIMP miracle", an important concept that can be translated mathematically as well. Indeed, because of the freeze-out scenario explained in Section 2.3, we can find an expression relating the actual abundance of DM  $\Omega_\chi$  with its annihilation cross section  $\langle\sigma_A v\rangle$  through Equation 2.12 [57].

$$\Omega_\chi h^2 \sim \frac{3 \cdot 10^{-27} \text{ cm}^3 \text{ s}^{-1}}{\langle\sigma_A v\rangle} \quad (2.12)$$

This equation implies that, since we do know the current abundance of DM in the Universe, the total annihilation cross section of DM should be equal to  $\sim 3 \cdot 10^{-26} \text{ cm}^3 \text{ s}^{-1}$ , which corresponds to the typical value given by WIMPs for a range of dark matter masses matching the expected one.

Several strategies can be used to detect such particles, as we will now see in the Section 2.5. This kind of particle basically arises in various BSM theories, such as the lightest supersymmetric particle in SUSY. According to this theory, each SM particle should have a superpartner whose quantum numbers would be identical except for their spins, which would differ by one half. All of these superpartners would then be new and undiscovered particles, giving us a perfect DM candidate, the neutralino  $\chi$ .

The WIMP are also interesting in the sense that introducing them in the terms of this supersymmetric theory would not only give us a DM candidate, but also solve the hierarchy problem, the apparent large discrepancy between multiple aspects of the weak and gravitational forces ( $10^{24}$  less times stronger).

## 2.5 Dark matter searches

As previously stated, several cosmological evidences allow us to introduce the concept of dark matter, but its properties such as its mass, coupling and interaction cross-section are difficult to study in this context. Several different ways can then be used in order to try and detect DM particles in order to study them, as represented in Figure 2.10, strategies which can usually be divided into three categories: the direct and indirect searches, mostly relying on the production of baryonic matter from the interaction between two DM particles or on the observation on the interaction between the dark and baryonic sector, and the production in colliders, usually able to probe lower DM candidates masses and which will actually be the main focus of this work. A discussion about these different detection strategies along with the main results obtained by different experiments in each case will

now be presented.

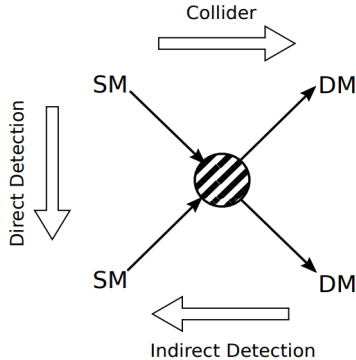


Figure 2.10: Schematic view of the three main DM detection strategies: direct, indirect and collider production searches [51].

### 2.5.1 Direct searches

From cosmological observations, we know that we live in a halo of dark matter. In this case, WIMPs should cross the Earth every day and, even if they interact only weakly, we should be able to directly detect them through their interaction with ordinary baryonic matter, for example because of their scattering with the nuclei of these particles. Indeed, the transfer of momentum between these two particles in this case might be detectable with the correct experimental device, typically placed deep underground to have the lowest possible background, which is the main source of perturbations of such experiments.

To study this particular category of searches, let's first of all introduce the rate of expected WIMP scattering off a target nucleus of mass  $m_N$  with Equation 2.13, rate which end up being described by a simple steeply falling exponential function as shown on Figure 2.11 [52], where  $E_{nr}$  is the nuclear recoil energy measured,  $m_\chi$  is the WIMP mass,  $\sigma$  its cross section,  $\rho_0 = 0.3 \text{ GeV cm}^{-3}$  is the local dark matter density and  $f(v)$  the normalized WIMP velocity distribution.

$$\frac{dR}{dE_{nr}} = \frac{\rho_0 M}{m_N m_\chi} \int_{v_{\min}}^{v_{\text{esc}}} v f(v) \frac{d\sigma}{dE_{nr}} dv \propto \exp\left(-\frac{E_{nr}}{E_0} \frac{4m_\chi m_N}{(m_\chi + m_N)^2}\right) \quad (2.13)$$

From this relation, the Equation 2.14 can be easily derived, representing this time the number of expected DM events in an experiment running during a time  $T$ , where  $\epsilon(E_{nr})$  is the efficiency of the detector for a given recoil energy.

$$N = T \int_{E_{\min}}^{E_{\max}} \epsilon(E_{nr}) \frac{dR}{dE_{nr}} dE_{nr} \quad (2.14)$$

The maximal velocity  $V_{\text{esc}}$  used as superior bound of the integral in 2.13 has actually been measured

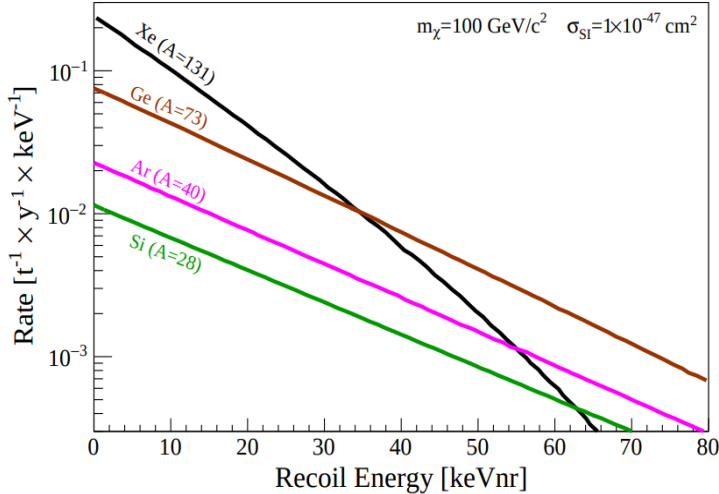


Figure 2.11: Nuclear recoil spectra induced in different materials for a given DM WIMP of 100 GeV, assuming a WIMP-nucleon Spin Independant (SI) cross section [52].

to be in the range [498 – 608] km/s at the 90% CL [53], since any particle having a velocity higher than this would not be bound any more to the gravitational potential of a galaxy. This has an important consequence: all the direct and indirect detection experiments actually need to take into account is the annual modulation of the observed count rate, due to the movement of the Earth around the Sun, as shown in Figure ?? [54], since this velocity is not negligible compared to the escape velocity  $V_{\text{esc}}$ .

From our perspective, it seems indeed that the velocity of the speed of WIMP particles arriving is changing depending on the month of the year, since the Earth is sometimes moving in the direction of the WIMP source, and is sometimes moving away: the maximal velocity is reached around June. This is extremely important to take into account this effect since, as we saw on the previous equations such as Equation 2.12, the count rate of incoming particles  $S(t)$  actually depends on this velocity, and this modulation then introduces a periodical modulation that we need to take into account, as shown in Equation 2.15, where the periodical part usually introduces a  $\sim 5\%$  deviation [52].

$$S(t) = B + S_0 + S_m \cos(\omega(t - t_0)) \quad (2.15)$$

This effect is also important because an experiment performed during a long period of time can actually help us finding an eventual hint of DM particles, since our signal is expected to follow this sinusoidal deviation while the background is expected to be constant. Moreover, this WIMP wind is expected to come from a particular region of the sky while the backgrounds are expected to be distributed uniformly, so this gives a way to isolate the signal.

Finally, it is also important to note that two different kinds of direct searches can be defined, depending on the category of the scattering between the DM and the nucleus: the Spin Independant

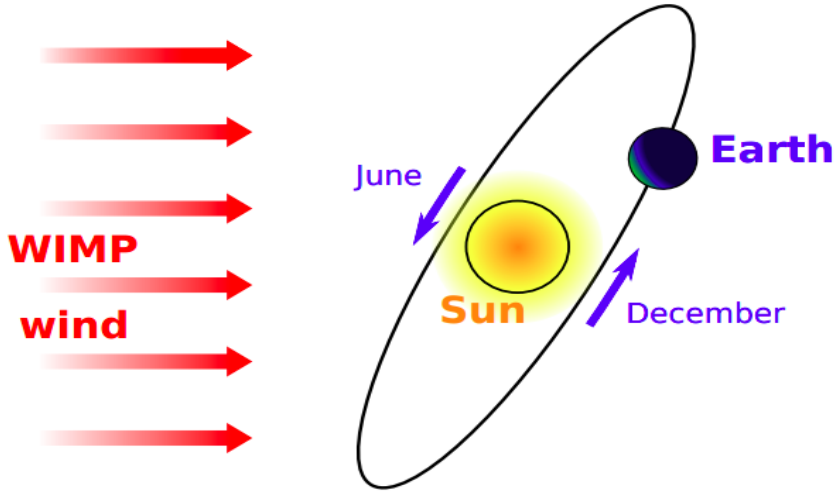


Figure 2.12: Schematic representation of the annual modulation of the WIMP wind introduced by the motion of rotation of the Earth around the Sun [54].

(SI) (proceeding through the scalar term) and Spin Dependant (SD) (proceeding through the axial term of the Lagragian) searches, since the interaction cross section  $\sigma$  of Equation 2.13 is expected to be different for DM particles having a spin 0 or not, as shown in Equation 2.16, where  $F$  is a factor accounting for the dependence of the scattering on the energy. This means that results obtained either hypothesis can usually not be compared with each other.

$$\frac{d\sigma}{dE_{nr}} \propto \sigma_{SI} F_{SI}^2(E_{nr}) + \sigma_{SD} F_{SD}^2(E_{nr}) \quad (2.16)$$

As previously stated, many experiments are dedicated to the direct search of DM particles, but in order to be isolate an eventual DM signal, an environment with an ultra-low background is usually required, which can usually be reduced either by placing the detector underground (to reduce the contamination due to the cosmic rays), by increasing the statistics or by choosing carefully the active material of the detector (to reduce the internal background coming from the detector itself). The impact these kind of parameters have on the final limits can be seen in Figure ??.

These detectors try to detect the scattering of an unknown exotic particle with an ordinary nucleus, which typically can give rise to different categories of signals. Some detectors try for example to detect the direct ionisation of the target atom, while others focus on the emission of light coming from the desexcitation of the scattered nucleus, and some even search for the heat produced by these collisions under the form of phonons in a crystal. All these different search strategies have been summarized schemtically in Figure 2.14.

As of today, no direct experiment has been able to detect serious hints for the existence of DM, and they have only been able to set limit on the scattering cross section depending on the models

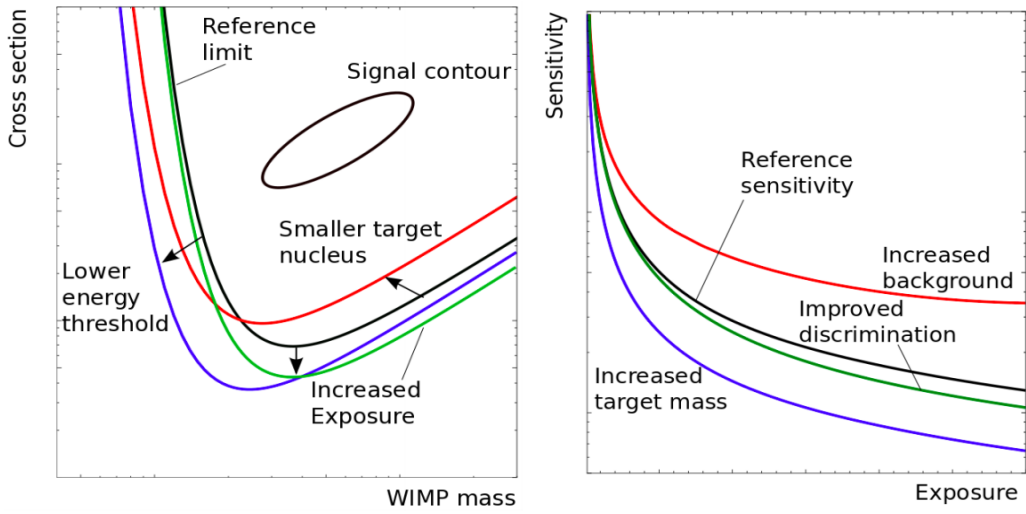


Figure 2.13: Impact of different experimental parameters on the final limits depending on the cross section and WIMP mass (on the left) or sensitivity and exposure (on the right), with respect to the expected limits (black curve) [55].

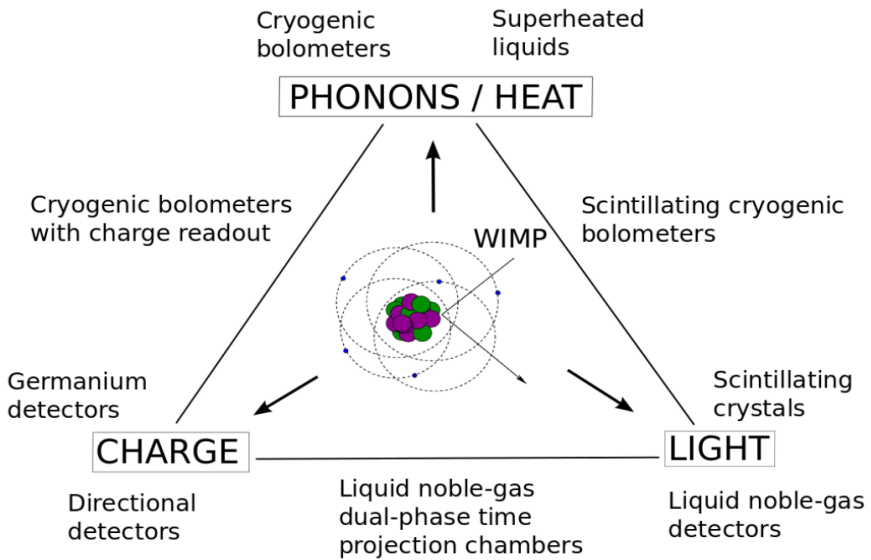


Figure 2.14: Schematic representation of the three main strategies to detect directly the recoil between DM particles and an ordinary nucleus [55].

parameters, as seen on Figure 2.16 for multiple experiments at once. However, the DAMA experiment at the LNGS underground laboratory did find an interesting result by showing the hints of an annual modulation signal compatible to the expected one due to the WIMP wind, in the 2-6 keV energy range, as seen on Figure 2.15 [56]. Further investigations about this modulation are still ongoing today, since no systematic effect able to account for the observed modulation amplitude and to simultaneously satisfy all the requirements of the signature has been found so far.

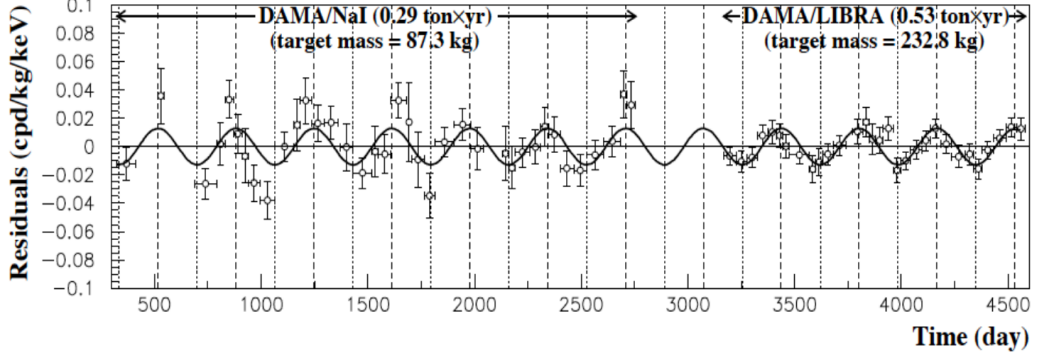


Figure 2.15: Observed and expected annual modulation in single hits events in the 2-6 keV energy range by the DAMA experiment [56].

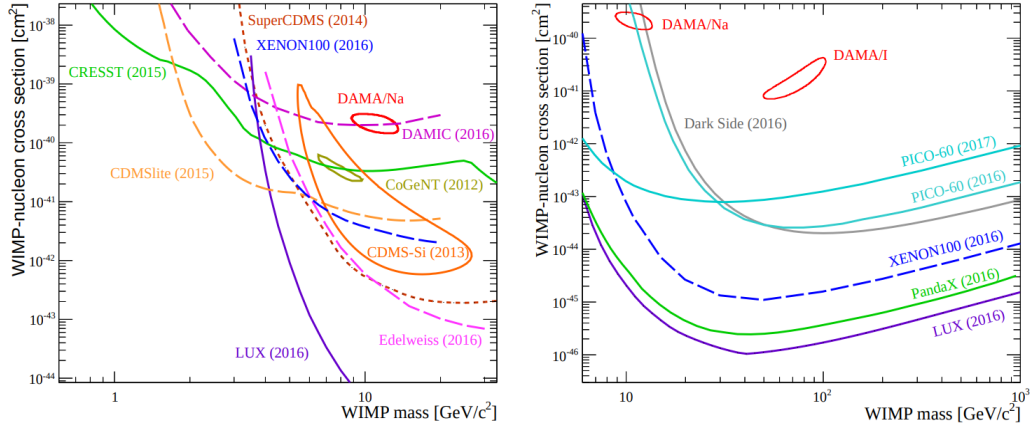


Figure 2.16: Exclusion limits obtained by various direct detection experiments considering a SI interaction cross section for low WIMP (on the left) or high WIMP masses (on the right) [55].

### 2.5.2 Indirect searches

The indirect detection of DM particles consists basically in searching for SM products coming from the annihilation of two DM particles or from its eventual direct decay, usually under the form of a flux of  $\gamma$ -rays, neutrinos, cosmic-rays or anti-matter appearing as an excess over the expected background. Indeed, many extensions to the SM, such as SUSY or Universal Extra Dimensions (UED) do provide solid DM candidates (the lightest supersymmetric particle and the lightest Kaluza-Klein state, respectively) expected to interact with each other, resulting in the immediate production

of SM (un)stable particles that can be detected by telescopes either placed on the ground or directly in space. Another point to make is that indirect searches are also affected by the annual fluctuation induced by the movement of the Earth around the Sun, as explained in the previous Section 2.5.1.

Indirect searches are actually extremely useful since it is sensitive to the DM its annihilation cross section, its mass and the density profile of DM halos  $\rho(\vec{r}(s, \Omega))$ , usually represented by a Navarro-Frenk-White (NFW) profile, as shown in Equation 2.17 [58], where  $r_s = 20$  kpc is the scale radius of the DM halo for the Milky Way and  $r$  is the distance to the center of the cluster considered, assumed to be spherical in this case.

$$\rho(r) \propto \frac{r_s}{r \cdot \left(1 + \frac{r}{r_s}\right)^2} \quad (2.17)$$

The flux coming from the annihilation of two DM particles is then expected to be proportional to its annihilation cross section  $\sigma v$ , the solid angle of observation  $\Omega$  and the number of particles emitted by this annihilation  $\frac{dN}{dE}$ , according to Equation 2.18, where the integration is done over the line of sight  $l$  and the solid angle of observation  $\Omega$ .

$$\frac{d\Phi}{d\Omega dE} = \frac{\sigma v}{8\pi m_\chi^2} \cdot \frac{dN}{dE} \iint_{l,\Omega} \rho^2(\vec{r}(s, \Omega)) dl d\Omega \equiv P \cdot J(\Delta\Omega) \quad (2.18)$$

This equation is extremely important for two reasons. First of all, it shows that, if a signal is found in direct detection, we could use this detection to determine the new object mass and scattering cross section and then use this information in order to obtain the DM density profile through Equation 2.18. The data obtained by the different strategies of detection are actually complementary. The second reason is that as we can see, the flux of incoming particles can actually be divided into two factors:  $P$ , entirely dependent on the physics of the DM particle, and the J-factor  $J(\Delta\Omega)$ , depending only on the distribution of DM within the system considered. This J-factor is in this sense actually a measurement of the quality of an astronomical object for an indirect measurement, since the higher the flux received, the better the measurement will be in general (even though this is not the only factor which matters, since for example the galactic center has a higher J-factor than the best dwarf galaxy observable, but also has a lot of backgrounds affecting the measurement).

As different channels of observations are available for us to analyze the eventual annihilation of DM, several strategies can be used in order to detect DM indirectly, as we will now see, by searching different kind of SM particles. Anyway, all these strategies have one goal in common: try to reduce the background, since the signal searched for is usually quite low while the uncertainties associated to the background in astrophysics is usually quite high.

## Through $\gamma$ -rays detection

The golden channel for such searches are through the production of  $\gamma$ -rays by DM annihilation  $\chi\chi \rightarrow \gamma + X$  or decay  $\chi \rightarrow \gamma + X$ , mainly because the energy scale of the WIMPs implies that most of the annihilation and decay radiation will be emitted in this range of energies, and because  $\gamma$ -rays are usually not deflecting when traveling to the observer (this means that the exact source of this kind of radiation can be easily and precisely pin-pointed). However, they do have one drawback as well: the Earth's atmosphere is usually opaque to this kind of radiation at this level of energy. This means that most of experiments searching for them simply cannot be performed from the ground and have to be sent to space.

One of the most famous detectors of this category is the so-called Fermi Large Telescope (LAT), a pair production detector launched in June 2008 and mostly sensitive to  $\gamma$ -rays between 20 MeV and 300 GeV [59]. This experiment has managed to exclude a large portion of the phase space, as seen in Figure 2.17. The GAMMA-400 experiment, whose launch is scheduled in 2020, will pick up the work of LAT, but studying a similar range but with a much improved angular and energy resolutions [60].

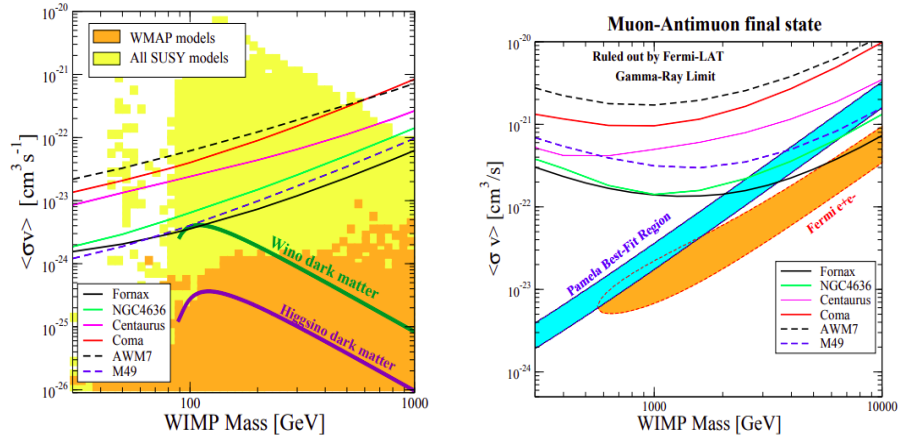


Figure 2.17: Upper limits on the DM annihilation cross section considering  $b\bar{b}$  (on the left) and a  $\mu^+\mu^-$  (on the right) final states as a function of the WIMP mass, for different clusters studied [59].

It is much harder for DM to produce high energy  $\gamma$ -rays and therefore, the flux of such particles decreases quite quickly with energy, making it harder to study since telescopes then need a much larger effective area to pick up the same quantity of signal, and have therefore to be put on the ground. Such telescope are called Imaging Atmospheric Cherenkov Telescopes (IACT) and have to take into account the atmospheric perturbation to work in an optimal way, but this kind of telescope is usually sensitive to a range of energies going from  $\sim 10$  GeV up to  $\sim 100$  TeV, but can usually only study a small degrees of the sky, forcing these experiments to choose carefully the objects to be studied. The Cherenkov Telescope Array (CTA) is a brand new telescope of this kind whose construction is supposed to start this year, that should improve greatly the sensitivity of high masses indirect DM searches.

## Through neutrinos detection

Interacting only weakly, neutrinos are another reliable source of data in the Universe since they are not supposed to be altered when traveling large distances, even though detecting neutrinos is usually much harder than detecting  $\gamma$ -rays and usually involves huge tanks of water in which neutrinos can produce a Cherenkov effect that will eventually be detected.

The most famous detector of this kind, the IceCube neutrino observatory, actually uses the ice of the South Pole instead of water to detect these particles with photodetectors, mainly because of the low interaction cross section of the neutrinos which then require the installation of a huge volume of material to increase the probability of interaction. Super-Kamiokande (Super-K), in Japan, is another large Cherenkov experiment dedicated to the detection of cosmic neutrinos. Both detectors are also largely involved as direct searches experiments, such they are also sensitive to the eventual recoil between DM and ordinary matter nuclei.

The problem with this kind of experiment is the difficulty of detection of neutrinos, along with the background levels from atmospheric neutrinos, as represented in Figure 2.18, typically several order of magnitude larger than the signal. Several strategies therefore need to be put in place in order to reduce the background level in such experiments, such as the study of the directionnality of the source and an appropriate choice of angle of observation, since most of the contamination is coming from tau neutrinos, themselves originating from muon neutrinos oscillation, strongly suppressed at the zenith.

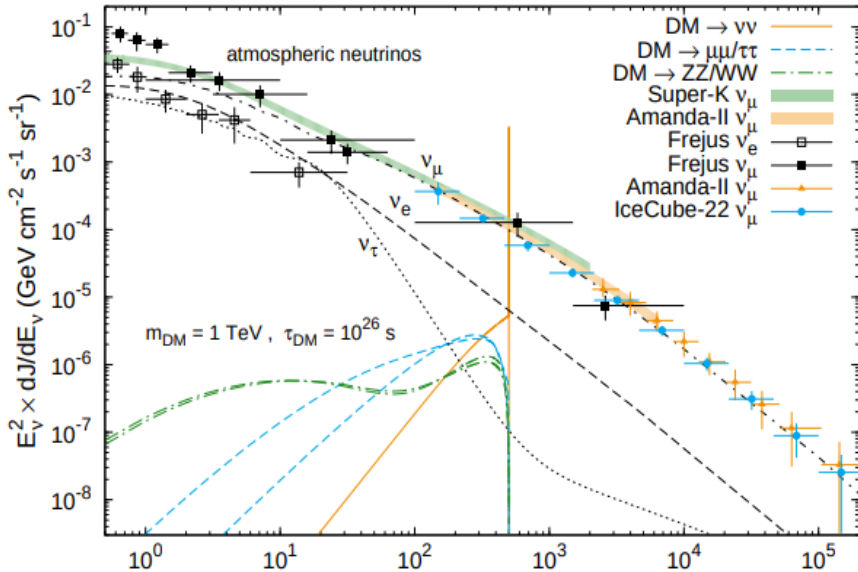


Figure 2.18: Neutrino spectra for a scalar DM candidate of 1 TeV for different indirect detection experiments and the corresponding background level expected [61].

### Through cosmic rays detection

Searching for anti-matter in the cosmic rays presents the advantage of being highly sensitive, because of the low levels of backgrounds this kind of searches implies. However, cosmic rays are affected when traveling through the Universe, and determining the exact location of their emission can be quite challenging.

Among the most famous detectors of this kind, we can quote PAMELA, a spatial telescope dedicated to the study of such cosmic rays since 2006. CERN's Alpha Magnetic Spectrometer (AMS), installed in the International Space Station has also studied such radiation from a range of a few hundred MeV up to 1 TeV. The data collected by this detector is compared to the exclusion limits obtained by the IceCube detector on Figure 2.19.

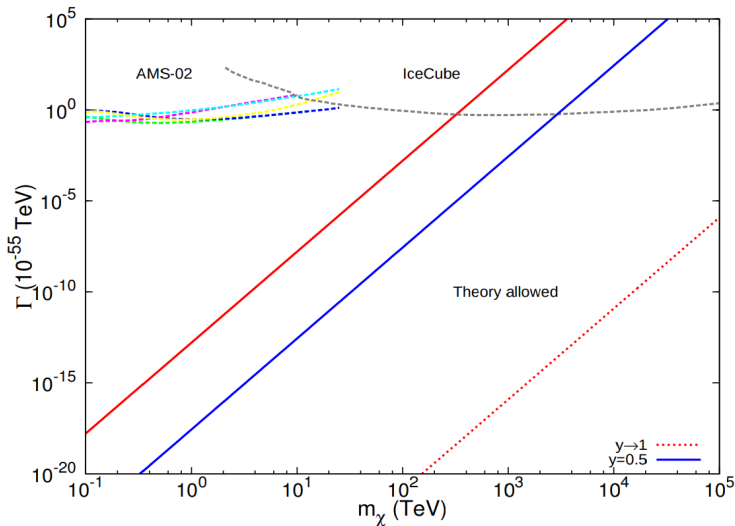


Figure 2.19: Limits of the decay width of the interaction with respect to the DM mass obtained by both IceCube and AMS [62].

### 2.5.3 Collider production

In this particular kind of searches, we are particularly interested in the eventual direct production of DM candidates following the collision between two highly energetic SM particles, a perfectly viable scenario if we keep assuming that DM should at least interact weakly with ordinary matter if we want to be able to produce or detect it in a laboratory.

In this case, different models for the interaction between SM and DM can be considered, each with a different level of complexity and different possible applications:

- The Effective Field Theory (EFT) approach is usually considered to be the easiest and most simplified one, even though it can still give us plenty of information about this kind of interactions. It relies on a strong assumption, assuming that the energy scale of the new exotic

physics is much larger than the actual energy accessible with our experiment, since the momentum transfer of this interaction needs to be much smaller than the mediator mass for this simplified approach to be valid.

According to this approach, represented in Figure 2.20, the interaction can be described using simplified operators (the most simple ones being either scalar  $\bar{\chi}\chi\bar{q}q$ , pseudoscalar  $\bar{\chi}\gamma^5\chi\bar{q}\gamma^5q$ , vector  $\bar{\chi}\gamma^\mu\chi\bar{q}\gamma_\mu q$  or axial-vector  $\bar{\chi}\gamma^\mu\gamma^5\chi\bar{q}\gamma_\mu\gamma^5q$ ) since, according to the assumption made, its mediator can usually be integrated out [51].

Despite of this strong assumption, this approach is actually quite useful anyway in the sense that it is able to provide us bounds on the new physics scale  $\Lambda$ , which can be related to the different couplings of the interaction as in Equation 2.19, where  $g_q$  and  $g_\chi$  are the coupling between the mediator and the SM or DM particle, and  $m_{\text{med}}$  is the mass of the mediator.

$$\frac{1}{\Lambda^2} = \frac{g_q g_\chi}{m_{\text{med}}} \quad (2.19)$$

additionally, direct searches experiments typically also introduce this kind of assumptions to extract constraints from their measurements, making it straightforward to compare the results obtained in both approaches. However, the transfer of momentum in the direct searches experiments is usually of the order of a few keV as seen in Equation 2.20, while in collider experiments such as the LHC this is of the order of  $\Theta(\text{GeV-TeV})$ .

$$E = \frac{m_\chi v_\chi^2}{2} \simeq 100 \text{ GeV} \cdot 10^{-6} \simeq 50 \text{ keV} \quad (2.20)$$

This means that, especially due to the increasing center of mass energy given by the LHC over the last few years, the basic EFT assumption is usually not respected and gives information about an out of reach phase space region anyway, making its usefulness quite relative in most cases. This is why more complex models need to be developed as well, such as the simplified models now introduced.

- The simplified models attempt to solve the issue related to the approximation made by the EFT approach, by increasing the level of details regarding the interaction between the dark and baryonic sectors. This is usually done by explicitly taking into account the mediator of the interaction, which can be considered of two different types in the context of this work: either scalar  $\phi$  or pseudoscalar  $a$  (both having a spin 0), described by the Lagrangians in Equation 2.21, considering the DM candidate to be a Dirac fermion coupling to the SM through the mediator considered and under the assumption of Minimal Flavour Violation (MFV). In this equation, the sum runs over the three SM families and the parameters  $y_i^f = \sqrt{2} \frac{m_i^f}{v}$  are the Yukawa couplings, much larger for the top quarks because of their mass, which will allow us to simplify the following equations [63].

$$\begin{cases} \mathcal{L}_{\text{fermion},\phi} \propto -g_\chi \phi \bar{\chi} \chi - \frac{\phi}{\sqrt{2}} \sum_i (g_u y_i^u \bar{u}_i u_i + g_d y_i^d \bar{d}_i d_i + g_l y_i^l \bar{l}_i l_i) \\ \mathcal{L}_{\text{fermion},a} \propto -ig_\chi a \bar{\chi} \gamma^5 \chi - \frac{ia}{\sqrt{2}} \sum_i (g_u y_i^u \bar{u}_i \gamma^5 u_i + g_d y_i^d \bar{d}_i \gamma^5 d_i + g_l y_i^l \bar{l}_i \gamma^5 l_i) \end{cases} \quad (2.21)$$

An important parameter in this case is the decay width of this mediator  $\Gamma_{\text{med}}$ , given by Equation 2.22 for either a scalar mediator  $\phi$  or Equation 2.23 for a pseudoscalar mediator  $a$ , where the first term corresponds to the mediator decay to SM particles, the second to its decay to DM particles and the last term its possible decay to gluons.

$$\begin{cases} \Gamma_\phi = \sum_f N_C \frac{y_f^2 g_\nu^2 m_\phi}{16\pi} \left(1 - \frac{4m_f^2}{m_\phi^2}\right)^{3/2} + \frac{g_\chi^2 m_\phi}{8\pi} \left(1 - \frac{4m_f^2}{m_\phi^2}\right)^{3/2} + \frac{\alpha_S^2 g_\nu^2 m_\phi^3}{32\pi^3 \nu^2} \left| f_\phi \left( \frac{4m_t^2}{m_\phi^2} \right) \right|^2 \\ f_\phi(\tau) = \tau \left( 1 + (1 - \tau) \arctan^2 \left( \frac{1}{\sqrt{\tau - 1}} \right) \right) \end{cases} \quad (2.22)$$

$$\begin{cases} \Gamma_a = \sum_f N_C \frac{y_f^2 g_\nu^2 m_a}{16\pi} \left(1 - \frac{4m_f^2}{m_a^2}\right)^{1/2} + \frac{g_\chi^2 m_a}{8\pi} \left(1 - \frac{4m_f^2}{m_a^2}\right)^{1/2} + \frac{\alpha_S^2 g_\nu^2 m_a^3}{32\pi^3 \nu^2} \left| f_a \left( \frac{4m_t^2}{m_a^2} \right) \right|^2 \\ f_a(\tau) = \tau \arctan^2 \left( \frac{1}{\sqrt{\tau - 1}} \right) \end{cases} \quad (2.23)$$

In the case of the simplified models, the minimal set of parameters describing the interaction is therefore  $\{m_\chi, m_{\text{med}}, g_\chi, g_q\}$ .

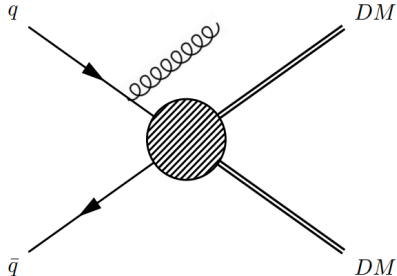


Figure 2.20: Schematic representation of a typical EFT modelization of an LHC event with an Initial State Radiation (ISR) object used to trigger the event [51].

An additional categorization of the DM production models can be done, by separating the so-called s-channel and t-channel models, as shown in Figure 2.21. In the first case, the most common one in collider searches, the mediator between the SM and DM is assumed to be a boson, and usually decays directly into a pair of DM particles. On the other hand, in the t-channel models, the mediator couples to one quark and one DM particle, with a colour exchange particle required. These models are relatively new and few dark matter searches have been performed using them so far.

In this work, simplified models with either scalar or pseudoscalar mediators will always be considered because of their relative simplicity and the lack of strong assumptions behind them. We will now study in particular the production and the search for DM within the LHC.

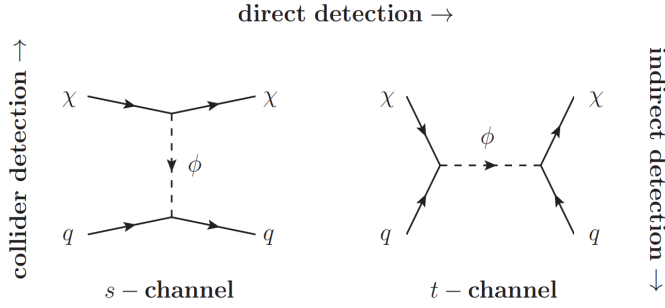


Figure 2.21: Schematic representation of a typical collider DM production through s-channel and t-channel processes [64].

## 2.6 DM production at the LHC

The Large Hadron Collider (LHC), colliding protons at a center of mass energy of 13 TeV, is actually a perfect machine to study such processes, because of the expected range of masses (100 GeV to 1 TeV) for the best DM candidates, as discussed in Section 2.3. However, since because of the weak interactions of such particles, they are not expected to interact at all with the detector, which will then basically search for missing transverse energy along with a SM particle triggering the event.

Several major categories of DM searches exist at the LHC, performed mainly by the CMS and ATLAS collaborations, depending on the strategy applied for such searches:

- First of all are the so-called **mono-X searches**, where X stands for a detectable SM particle used to trigger the event while the DM mediator usually decays into a pair of particles escaping the detector, leaving behind some Missing Transverse Energy (MET), a key variable to all these searches, as shown in Figure 2.22. Depending on the nature of the X particle, several searches can be performed: we can for example mention the mono- $\gamma$  [65, 66] or mono-jet [67, 68] 13 TeV searches performed by the ATLAS and CMS collaborations.

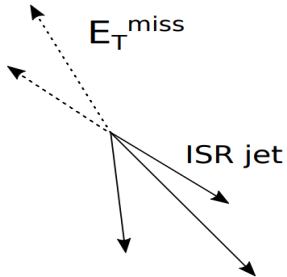


Figure 2.22: Schematic representation of a typical mono-X event, with an ISR jet in this case going back-to-back with some MET [51].

Additionally, if the DM mass is high enough, a coupling to the Higgs boson is also possible, or an eventual decay of the Higgs itself to a couple of DM particles  $H \rightarrow \chi\bar{\chi}$  is kinematically not

impossible. This channel, known as the mono-Higgs searches is sensitive to all the decays of the Higgs, even though the searches excluding most of the phase spaces are performed using the  $H \rightarrow b\bar{b}$  and  $H \rightarrow \gamma\gamma$  decay because of their branching ratios [69, 70].

- Then, we can find the searches for DM production in **association with heavy quark(s)**. This particular search for DM produced in association with one or two quark pairs can be typically quoted within this category and will be detailed in the next section, but other analyses such as the one probing the  $b\bar{b} + \text{DM}$  to its different final states depending on the decay of the bottom quark also belongs to this group, at 8 or 13 TeV [14, 18].

These searches have to combine the discriminant power of several variables to separate the signal from the backgrounds, since the MET distribution on its own is usually not enough, but they present the advantage of being favoured by the higher Yukawa coupling to more massive particles implied by the MFV assumption.

- **Dijet searches** are also an important part of the work being performed using the LHC data, and actually provide the best exclusion limits for most the spin-1 mediated models considered (up to a few TeV for typical coupling choices) [71, 72]. In this case, the sensitivity is obtained by searching for either narrow or large resonances on the exponentially falling QCD background, while the other searches were mostly dedicated in searching for bumps in the MET spectrum.
- **Supersymmetric searches** can also be performed to search for DM, SUSY which would solve the hierarchy problem while giving us perfect DM candidates such as the neutralino  $\chi$ , the lightest stable supersymmetric particle, obtained in many of the MSSM theories, having an hypothetic mass below the TeV scale [73].
- The **Higgs portal** to the dark sector is another interesting strategy. In some specific cases, when considering spin-0 mediated interactions between the dark and baryonic sectors, the Higgs could be considered as the mediator of the interaction as well, which only require a minimal modification of the SM lagragian. It is then necessary to study the different Higgs production modes, such as the gluon fusion and Vector Boson Fusion (VBF) mechanisms, to search for an eventual invisible decay of the Higgs into a couple of DM particles, assuming that its mass is lower than  $\sim 62.5$  GeV,  $m_H/2$  [74].
- Finally, and this is quite new, **long-lived searches** can also be performed. These are interested because they can extend the current searches performed to also consider the eventual creation of long-lived particles which would decay a few centimeters further than the primary vertex of the proton-proton collision [75]. Typical SM signatures do not usually include such events, making this channel relatively background-free, even though the reconstruction of the different objects is much harder in this case.

All the results obtained the different searches performed by the CMS collaboration using the full 2016 dataset can be summarized in Figure 2.23 for spin-0 mediators and in Figure 2.24 when considering spin-1 mediators. These results have also been compared to the results obtained by several direct detection experiments in Figure 2.25, considering both the Spin Dependant (SD) and Spin Independant (SI) cases, as explained in Section 2.5.1.

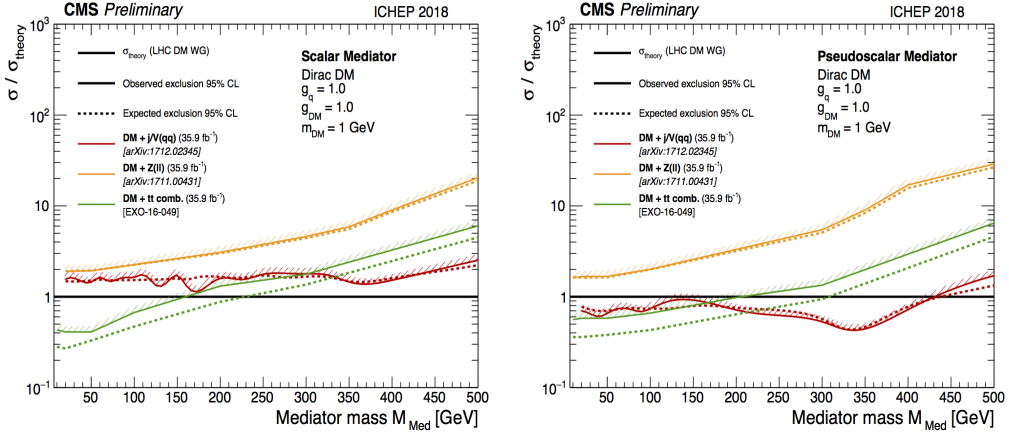


Figure 2.23: Observed and expected 95% exclusion limits obtained by different searches of the CMS collaboration as a function the spin-0 mediator, considering a scalar (on the left) and pseudoscalar (on the right) interaction.

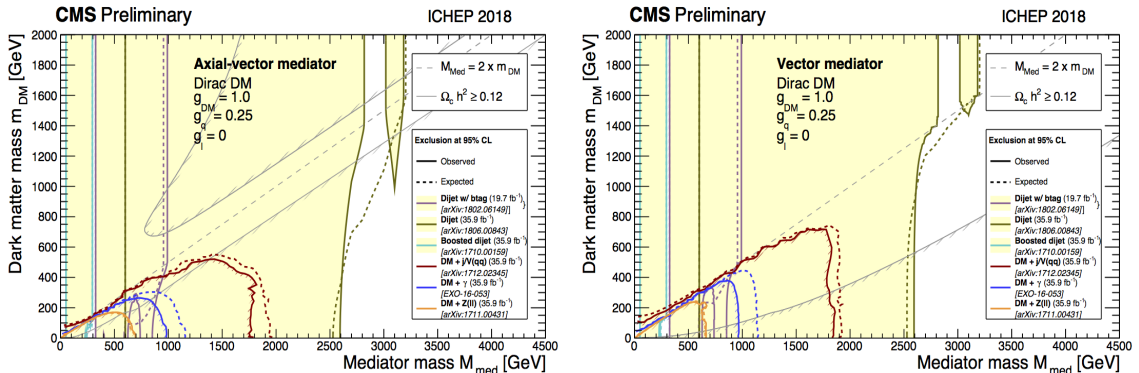


Figure 2.24: Observed and expected 95% exclusion limits obtained by different searches of the CMS collaboration as a function the spin-1 mediator, considering an axial-vector (on the left) and axial (on the right) interaction.

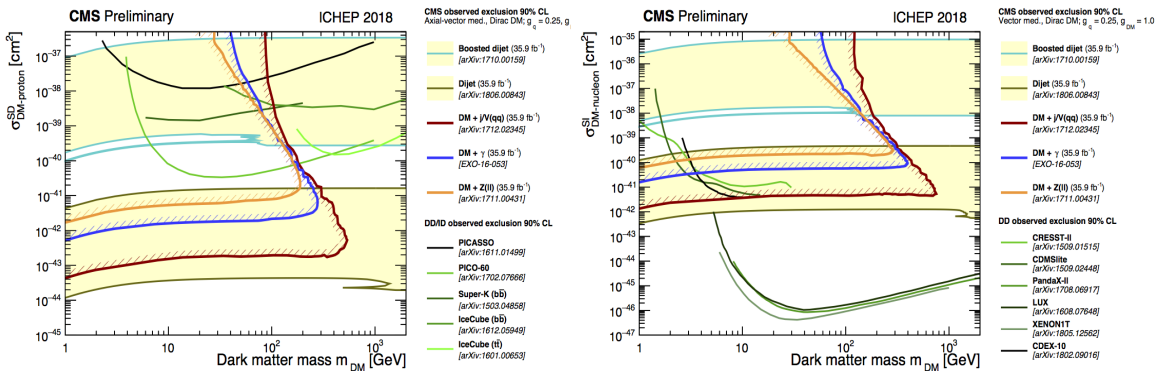


Figure 2.25: CMS 90% exclusion limits compared to the most famous direct detection experiments for the SD (on the left) and SI (on the right) scenarios, obtained using similar couplings.

This particular analysis and our signal of interest, the search for DM production in addition with a single or a pair of top quarks falls into the second category and will now be detailed. It is already important to note that this analysis has been performed considering the DM candidate to be a Dirac fermion with all the couplings equal and set to 1, as recommended by the Dark Matter Working Group (DMWG) [76].

### 2.6.1 The single top production channel

### 2.6.2 The $t\bar{t}$ production channel

All masses considered

### 2.6.3 The dilepton final state

## 2.7 Previous relevant results

This analysis being performed at a center of mass energy  $\sqrt{s} = 13$  TeV, only the most relevant results to this particular energy and previously obtained by both the CMS and ATLAS collaborations of CERN will be quoted here.

First of all, the **ATLAS collaboration** published interesting results at this center of mass energy, considering an integrated luminosity of  $13.3 \text{ fb}^{-1}$ , and obtained the corresponding exclusion limits at the 95% CL, considering the  $t\bar{t}+\text{DM}$  model and both scalar and pseudoscalar spin-0 mediators for the interaction, as shown in Figure 2.26. In this case, and for the couplings considered, an exclusion up to  $\sim 375$  GeV has been achieved.

Considering the full 2016 dataset of  $36.1 \text{ fb}^{-1}$ , similar results have been obtained by the ATLAS collaboration, as shown in Figure 2.27. In this case, and for lower coupling values, an exclusion up to around 100 GeV has been obtained considering scalar and pseudoscalar mediators.

The **CMS collaboration** published in 2018 a similar analysis, but using only the  $35.9 \text{ fb}^{-1}$  of data collected during the year 2016. This analysis combined the three different final states possible (hadronic, semileptonic and dileptonic) and computed the limits on the signal strength for different mediator and dark matter masses, considering both scalar and pseudoscalar mediators [20]. The results obtained can be found in Figure ??.

Last year, a combination of the  $t/\bar{t}+\text{DM}$  and  $t\bar{t}+\text{DM}$  analyses has also been published [21], combining this time only the hadronic and semileptonic channels of both analyses. The limits obtained in this case are represented in Figure 2.28, where the limits obtained by each analysis on their own along with the results of the combination, leading to a factor 2 improvement of the results, have been

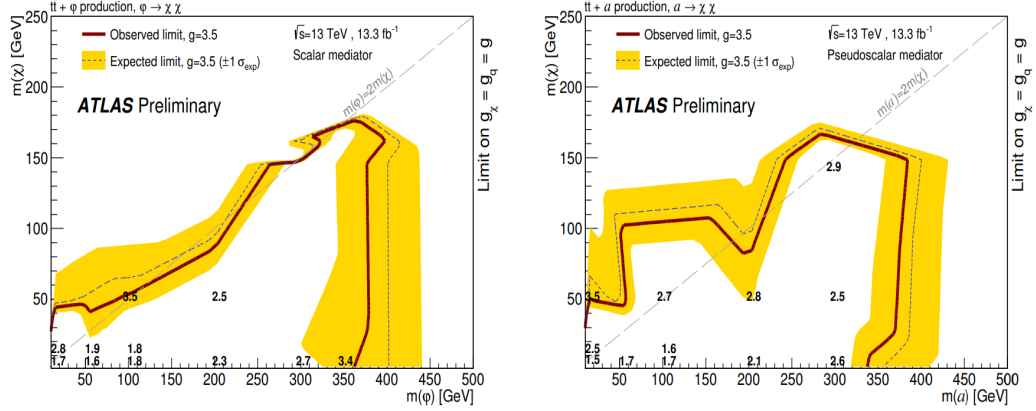


Figure 2.26: Limits on the mass on the DM and mediator masses obtained by ATLAS using 13.3 fb $^{-1}$  of 13 TeV data, considering scalar (on the left) and pseudoscalar (on the right) mediators [15].

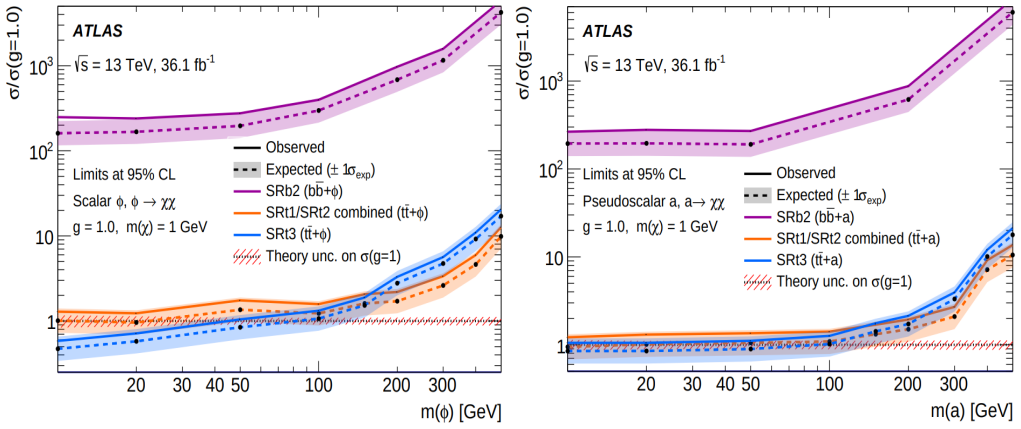


Figure 2.27: Exclusion limits at the 95% CL obtained by ATLAS considering scalar (on the left) and pseudoscalar (on the right) mediators, for a DM mass of 1 GeV [18]

represented.

This combination managed to exclude the production of scalar mediators up to 290 GeV and pseudoscalar mediators up to 300 GeV, at the 95% CL for the couplings considered. This combined analysis actually lead to the most stringent exclusion limits of the LHC on the production of DM through these categories of spin-0 mediators.

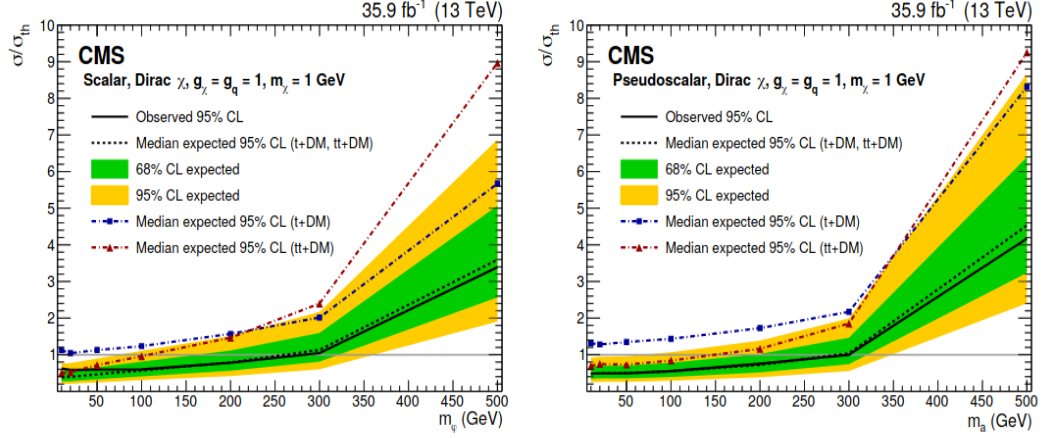


Figure 2.28: Expected and observed 95% CL limits on the DM production cross sections shown considering scalar (on the left) and pseudoscalar (on the right) mediators for the interaction [21].



# Chapter 3

## The experimental device

### 3.1 The LHC accelerator

### 3.2 The CMS detector

#### 3.2.1 Tracker

#### 3.2.2 Electromagnetic calorimeter

#### 3.2.3 Hadronic calorimeter

#### 3.2.4 Muon system

#### 3.2.5 Trigger

#### 3.2.6 Data acquisition



# Chapter 4

## Objects reconstruction

### 4.1 Particle Flow algorithm

### 4.2 Leptons reconstruction

#### 4.2.1 Electrons

#### 4.2.2 Muons

### 4.3 Jets reconstruction

#### 4.3.1 B-tagging

### 4.4 Missing transverse energy

### 4.5 Top reconstruction



# Chapter 5

## Data, signals and backgrounds

### 5.1 Data samples

### 5.2 Signal samples

### 5.3 Background prediction

#### 5.3.1 The main background: $t\bar{t}$

#### 5.3.2 Drell-Yan estimation

#### 5.3.3 Non prompt contamination

#### 5.3.4 Smaller backgrounds

#### 5.3.5 Weights and corrections applied



# Chapter 6

## Event selection

### 6.1 Signal regions

### 6.2 Control regions

### 6.3 Background-signal discrimination

#### 6.3.1 Discriminating variables

#### 6.3.2 Neural network



# Chapter 7

## Results and interpretations

### 7.1 Systematics and uncertainties

### 7.2 Results



# Chapter 8

## Conclusions

### 8.1 Future prospects



# Appendices



# List of figures

2.1	Expected and observed rotation curves of the galaxy NGC 6503 [6]. The black dots correspond to the data and the <i>luminous</i> line corresponds to the expected rotation curve. . . . .	7
2.2	Anisotropies in the temperature of the CMB, as observed by the Planck satellite in 2018 [27]. . . . .	8
2.3	Power spectrum of the CMB obtained by Planck, representing the fluctuations of the temperature of this radiation with respect to the angular angle of observation. . . .	9
2.4	Mass distributions obtained by the Magellan in the visible (on the left) and Chandra on the X-rays spectrum (on the right) telescopes of the Bullet Cluster, yet another clear evidence for the existence of DM [31]. . . . .	10
2.5	Computer simulations for cold (on the left) and warm (on the right) DM scenarios and their impact on a galactic halo at 0 redshift [33]. . . . .	12
2.6	Halo fraction upper limit at the 95% CL compared to the mass of the lensing object for different MACHO models considered by the EROS (on the top) and the MACHO (on the bottom) collaborations [38]. . . . .	14
2.7	Neutrino cross section from the charged current as measured by different experiments over a large range of energies, for both neutrinos $\nu$ and antineutrinos $\bar{\nu}$ [39]. . . .	15
2.8	3.57 keV emission line detected with a $4.5\sigma$ CL by the XMM-Newton telescope in 2014, which could be a hint of the presence of DM [43]. . . . .	16
2.9	Axion exclusion plot summary and projected coverage of actual experiments [49]. . .	17
2.10	Schematic view of the three main DM detection strategies: direct, indirect and collider production searches [51]. . . . .	19
2.11	Nuclear recoil spectra induced in different materials for a given DM WIMP of 100 GeV, assuming a WIMP-nucleon SI cross section [52]. . . . .	20
2.12	Schematic representation of the annual modulation of the WIMP wind introduced by the motion of rotation of the Earth around the Sun [54]. . . . .	21

2.13	Impact of different experimental parameters on the final limits depending on the cross section and WIMP mass (on the left) or sensitivity and exposure (on the right), wth respect to the expecd limits (black curve) [55]. . . . .	22
2.14	Schematic representation of the three main strategies to detect directly the recoil between DM particles and an ordinary nucleus [55]. . . . .	22
2.15	Observed and expected annual modulation in single hits events in the 2-6 keV energy range by the DAMA experiment [56]. . . . .	23
2.16	Exclusion limits obtained by various direct detection experiments considering a SI interaction cross section for low WIMP (on the left) or high WIMP masses (on the right) [55]. . . . .	23
2.17	Upper limits on the DM annihilation cross section considering $b\bar{b}$ (on the state) and a $\mu^+\mu^-$ (on the right) final states as a function of the WIMP mass, for different clusters studied [59]. . . . .	25
2.18	Neutrino spectra for a scalar DM candidate of 1 TeV for different indirect detection experiments and the corresponding background level expected [61]. . . . .	26
2.19	Limits of the decay width of the interaction with respect to the DM mass obtained by both IceCube and AMS [62]. . . . .	27
2.20	Schematic representation of a typical EFT modelization of an LHC event with an ISR object used to trigger the event [51]. . . . .	29
2.21	Schematic representation of a typical collider DM production through s-channel and t-channel processes [64]. . . . .	30
2.22	Schematic representation of a typical mono-X event, with anISR jet in this case going back-to-back with some MET [51]. . . . .	30
2.23	Observed and expected 95% exclusion limits obtained by different searches of the CMS collaboration as a function the spin-0 mediator, considering a scalar (on the left) and pseudoscalar (on the right) interaction. . . . .	32
2.24	Observed and expected 95% exclusion limits obtained by different searches of the CMS collaboration as a function the spin-1 mediator, considering an axial-vector (on the left) and axial (on the right) interaction. . . . .	32
2.25	CMS 90% exclusion limits compared to the most famous direct detection experiments for the SD (on the left) and SI (on the right) scenarios, obtained using similar couplings. . . . .	32
2.26	Limits on the mass on the DM and mediator masses obtained by ATLAS using 13.3 fb $^{-1}$ of 13 TeV data, considering scalar (on the left) and pseudoscalar (on the right) mediators [15]. . . . .	34

2.27 Exclusion limits at the 95% CL obtained by ATLAS considering scalar (on the left) and pseudoscalar (on the right) mediators, for a DM mass of 1 GeV [18] . . . . .	34
2.28 Expected and observed 95% CL limits on the DM production cross sections shown considering scalar (on the left) and pseudoscalar (on the right) mediators for the interaction [21]. . . . .	35



## **List of tables**



# Bibliography

- [1] F. Englert and R. Brout, "Broken symmetry and the mass of gauge vector mesons", Phys. Rev. Lett. 13, pp. 321-323, 1964
- [2] P. W. Higgs, "Broken symmetries and the masses of gauge bosons", Phys. Rev. Lett. 13, pp. 508-509, 1964
- [3] S. Chatrchyan et al., "Observation of a new boson at a mass of 125 GeV with the CMS experiment at the LHC", Phys. Lett. B716, pp. 30-61, 2012 [arXiv: 1207.7235]
- [4] G. Aad et al., "Observation of a new particle in the search for the Standard Model Higgs boson with the ATLAS detector at the LHC", Phys. Lett. B716, pp. 1-29, 2012 [arXiv: 1207.7214]
- [5] V.C. Rubin, W.K. Ford and N. Thonnard, "Rotational properties of 21 SC galaxies with a large range of luminosities and radii, from NGC 4605 ( $R=4\text{kpc}$ ) to UGC 2885 ( $R=122\text{kpc}$ )", Astrophysical Journal 238, pp. 471-487, 1980
- [6] K.G. Begeman, A.H. Broeils and R.H. Sanders, "Extended rotation curves of spiral galaxies - Dark haloes and modified dynamics", Monthly Notices of the Royal Astronomical Society, vol. 249, issue 3, ISSN 0035-8711, 1991
- [7] A. Robertson, R. Massey and V. EkCMBTemperaturee, "What does the Bullet Cluster tell us about self-interacting dark matter?", Monthly Notices of the Royal Astronomical Society, vol. 465, issue 1, 2017 [arXiv: 1605.04307]
- [8] J.B. Mu?oz, C. Dvorkin and A. Loeb, "21-cm Fluctuations from Charged Dark Matter", Phys. Rev. Lett. 121, 121301 (2018) [arXiv: 1804.01092]
- [9] A. Natarajan, "A closer look at CMB constraints on WIMP dark matter", Phys. Rev. D85, 2012 [arXiv:1201.3939 ]
- [10] G. D'Ambrosio G.F. Giudice, G. Isidori and A. Strumia, "Minimal Flavour Violation: an effective field theory approach", Nucl.Phys. 645, pp 155-187, 2002 [arXiv:0207.036 ]
- [11] M. Tanabashi et al., Particle Data Group, Phys. Rev. D98, 030001 (2018)
- [12] CMS Collaboration, "Search for the production of dark matter in association with top-quark pairs in the single-lepton final state in proton-proton collisions at  $\sqrt{s} = 8 \text{ TeV}$ ", JHEP, vol. 6 121, 2015

- [13] CMS Collaboration,, "Search for the Production of Dark Matter in Association with Top Quark Pairs in the Di-lepton Final State in pp collisions at  $\sqrt{s} = 8$  TeV", CMS-PAS-B2G-13-004, 2014
- [14] "Search for dark matter in events with heavy quarks and missing transverse momentum in pp collisions with the ATLAS detector", Eur. Phys. J. C (2015) 75:92
- [15] ATLAS Collaboration, Search for the Supersymmetric Partner of the Top Quark in the Jets+Emiss Final State at  $\sqrt{s} = 13$  TeV", ATLAS-CONF-2016-077
- [16] ATLAS Collaboration, "Search for top squarks in final states with one isolated lepton, jets, and missing transverse momentum in  $\sqrt{s} = 13$  TeV pp collisions with the ATLAS detector", ATLAS-CONF-2016-050, 2016
- [17] ATLAS Collaboration, "Search for direct top squark pair production and dark matter production in final states with two leptons in  $\sqrt{s} = 13$  TeV pp collisions using  $13.3 \text{ fb}^{-1}$  of ATLAS data", ATLAS-CONF-2016-076, 2016
- [18] ATLAS Collaboration, "Search for dark matter produced in association with bottom or top quarks in  $\sqrt{s} = 13$  TeV pp collisions with the ATLAS detector", Eur. Phys. J. C 78 (2018) 18 [arXiv: 1710.11412]
- [19] CMS Collaboration, Search for dark matter produced in association with heavy-flavor quark pairs in proton-proton collisions at  $\sqrt{s} = 13$  TeV", Eur. Phys. J. C (2017) 77: 845
- [20] CMS Collaboration, "Search for dark matter particles produced in association with a top quark pair at  $\sqrt{s} = 13$  TeV", Phys. Rev. Lett. 122, 011803 (2019) [arXiv: 1807.06522]
- [21] CMS Collaboration, "Search for dark matter produced in association with a single top quark or a top quark pair in proton-proton collisions at  $\sqrt{s} = 13$  TeV", JHEP, vol. 03 141, 2019 [arXiv: 1901.01553]
- [22] F. Zwicky, "Die Rotverschiebung von extragalaktischen Nebeln", Helvetica Physica Acta , vol. 6, pp. 110-127, 1933
- [23] S. Van den Bergh, Phys Rev D "The early history of dark matter", Dominion Astrophysical Observatory, 1999
- [24] V.C. Rubin, W.K. Ford, "Rotation of the Andromeda Nebula from a Spectroscopic Survey of Emission Regions", Astrophysical Journal 159, p. 379, 1970
- [25] A. A. Penzias, R.W. Wilson, "A Measurement of Excess Antenna Temperature at 4080 Mc/s", Astrophysical Journal 142, pp. 419-421
- [26] D.J. Fixsen, "The temperature of the cosmic microwave background", Astrophysical Journal, 2009
- [27] Planck Collaboration, "Planck 2018 results. I. Overview and the cosmological legacy of Planck", 2018 [arXiv: 1807.06205]

- [28] R. Tojeiro, "Understanding the Cosmic Microwave Background Temperature Power Spectrum", 2006
- [29] Planck Collaboration, "Planck 2018 results. VI. Cosmological parameters", 2018 [arXiv: 1807.06209]
- [30] "Astrophysical Constants and Parameters", 2019
- [31] D. Clowe et all., "A Direct Empirical Proof of the Existence of Dark Matter", *Astrophysical Journal Letters* 648, 2006
- [32] K.R. Dienes, J. Fennick, J. Kumar, B. Thomas "Dynamical Dark Matter from Thermal Freeze-Out", *Phys. Rev. D* 97, 063522 (2018) [arXiv: 1712.09919]
- [33] C.S. Frenk, S.D.M. White, "Dark matter and cosmic structure", *Annalen der Physik*, p. 22 , 2012 [arXiv: 1210.0544]
- [34] R. Kirk, "Dark matter genesis"
- [35] M. Drewes et all., "A White Paper on keV Sterile Neutrino Dark Matter", 2016 [arXiv: 1602.04816]
- [36] C. Alcock et all., "The MACHO Project: Microlensing Results from 5.7 Years of LMC Observations", *Astrophys.J.* 542 (2000) 281-307
- [37] P. Tisserand et all., "Limits on the Macho content of the Galactic Halo from the EROS-2 Survey of the Magellanic Clouds", *A & A* 469, pp. 387-404 (2007)
- [38] EROS and MACHO collaborations, "EROS and MACHO Combined Limits on Planetary Mass Dark Matter in the Galactic Halo", 1998
- [39] Particle Data Group, "Neutrino Cross Section Measurements", PDG 2019
- [40] K. McFarland, "Neutrino Interactions", 2008 [arXiv: 0804.3899]
- [41] E. Morgante, "Aspects of WIMP Dark Matter Searches at Colliders and Other Probes", Springer theses, 2016
- [42] F. Couchot et all., "Cosmological constraints on the neutrino mass including systematic uncertainties", *A & A* 606, A104 (2017)
- [43] E. Bulbul et all., "Detection of An Unidentified Emission Line in the Stacked X-ray spectrum of Galaxy Clusters", 2014 [arXiv: 1402.2301]
- [44] A. Boyarsky et all., "An unidentified line in X-ray spectra of the Andromeda galaxy and Perseus galaxy cluster", *Phys. Rev. Lett.* 113, 251301 (2014) [arXiv: 1402.4119]
- [45] A. Boyarsky et all., "Checking the dark matter origin of 3.53 keV line with the Milky Way center", *Phys. Rev. Lett.* 115, 161301 (2015) [arXiv: 1408.2503]
- [46] T. Jeltema1 and S. Profumo, "Deep XMM Observations of Draco rule out at the 99% Confidence Level a Dark Matter Decay Origin for the 3.5 keV Line", 2015 [arXiv: 1512.01239]

- [47] D. Wu, "A Brief Introduction to the Strong CP Problem", Superconducting Super Collider Laboratory, 1991
- [48] R.D. Peccei, H.R. Quinn, "CP Conservation in the Presence of Pseudoparticles", Phys. Rev. Lett. 38, 1440, 1977
- [49] P.W. Graham et all., "Experimental Searches for the Axion and Axion-like Particles", Annual Review of Nuclear and Particle Science 65, 2015 [arXiv: 1602.00039]
- [50] CAST collaboration, "New CAST limit on the axion-photon interaction", Nature Physics 13, pp. 584-590 (2017)
- [51] B. Penning, "The Pursuit of Dark Matter at Colliders - An Overview", 2017 [arXiv: 1712.01391]
- [52] M. Schumann, "Direct Detection of WIMP Dark Matter: Concepts and Status", J. Phys. G46 (2019) no.10, 103003 [arXiv: 1903.03026]
- [53] S.C. Martin et all., "The RAVE survey: constraining the local Galactic escape speed", Mon.Not.Roy.Astron.Soc.379:755-772, 2007
- [54] K. Freese, M. Lisanti, C. Savage, "Annual Modulation of Dark Matter: A Review", [arXiv: 1209.3339v3]
- [55] T.M. Undagoitia and L. Rauch, "Dark matter direct-detection experiments", J. Phys. G43 (2016) no.1, 013001 [arXiv: 1509.08767]
- [56] R. Bernabei et all., "First results from DAMA/LIBRA and the combined results with DAMA/NaI", Eur.Phys.J.C56:333-355, 2008 [arXiv: 0804.2741]
- [57] J.M. Gaskins, "A review of indirect searches for particle dark matter", Contemporary Physics, 2016 [arXiv: 1604.00014]
- [58] F.S. Queiroz, "Dark Matter Overview: Collider, Direct and Indirect Detection Searches", Max-Planck Institute of Physics
- [59] LAT collaboration, "Constraints on Dark Matter Annihilation in Clusters of Galaxies with the Fermi Large Area Telescope", JCAP 05(2010)025 [arXiv: 1002.2239]
- [60] A.A. Moiseev et all., "Dark Matter Search Perspectives with GAMMA-400", 2013 [arXiv: 1307.2345]
- [61] L. Covi et all., "Neutrino Signals from Dark Matter Decay", JCAP 1004:017, 2010 [arXiv: 0912.3521]
- [62] B. Lu and H. Zong, "Limits on the Dark Matter from AMS-02 antiproton and positron fraction data", Phys. Rev. D 93, 103517 (2016) [arXiv: 1510.04032]
- [63] J. Abdallah et all., "Simplified Models for Dark Matter Searches at the LHC", Phys. Dark Univ. 9-10 (2015) 8-23 [arXiv: 1506.03116]

- [64] H. An, L. Wang, H. Zhang, "Dark matter with t-channel mediator: a simple step beyond contact interaction", Phys. Rev. D 89, 115014 (2014) [arXiv: 1308.0592]
- [65] ATLAS Collaboration, "Search for dark matter and other new phenomena in events with an energetic jet and large missing transverse momentum using the ATLAS detector", JHEP 01 (2018) 126 [arXiv: 1711.03301]
- [66] CMS Collaboration, "Search for new physics in the monophoton final state in proton-proton collisions at  $\sqrt{s} = 13$  TeV", J. High Energy Phys. 10 (2017) 073 [arXiv: 1706.03794]
- [67] CMS Collaboration, "Search for dark matter produced with an energetic jet or a hadronically decaying W or Z boson at  $\sqrt{s} = 13$  TeV", JHEP 07 (2017) 014 [arXiv: 1703.01651]
- [68] CMS Collaboration, "Search for new physics in final states with an energetic jet or a hadronically decaying W or Z boson and transverse momentum imbalance at  $\sqrt{s} = 13$  TeV", Phys. Rev. D 97, 092005 (2018) [arXiv: 1712.02345]
- [69] ATLAS Collaboration, "Search for dark matter in association with a Higgs boson decaying to two photons at  $\sqrt{s} = 13$  TeV with the ATLAS detector", Phys. Rev. D 96 (2017) 112004 [arXiv: 1706.03948]
- [70] CMS Collaboration, "Search for associated production of dark matter with a Higgs boson decaying to  $b\bar{b}$  or  $\gamma\gamma$  at  $\sqrt{s} = 13$  TeV", JHEP 10 (2017) 180 [arXiv: 1703.05236]
- [71] Atlas Collaboration, "Search for new phenomena in dijet events using 37 fb<sup>-1</sup> of pp collision data collected at  $\sqrt{s} = 13$  TeV with the ATLAS detector", Phys. Rev. D 96, 052004 (2017) [arXiv: 1703.09127]
- [72] CMS Collaboration, "Search for narrow and broad dijet resonances in proton-proton collisions at  $\sqrt{s} = 13$  TeV and constraints on dark matter mediators and other new particles", JHEP 08 (2018) 130 [arXiv: 1806.00843]
- [73] C. Munoz, "Models of Supersymmetry for Dark Matter", FTUAM 17/2, IFT-UAM/CSIC-17-005, 2017 [arXiv: 1701.05259]
- [74] CMS Collaboration, "Searches for invisible decays of the Higgs boson in pp collisions at  $\sqrt{s} = 7, 8,$  and  $13$  TeV", JHEP 02 (2017) 135 [arXiv: 1610.09218]
- [75] J. Alimena et all., "Searching for long-lived particles beyond the Standard Model at the Large Hadron Collider", 2019 [arXiv: 1903.04497]
- [76] A. Albert et all., "Recommendations of the LHC Dark Matter Working Group: Comparing LHC searches for heavy mediators of dark matter production in visible and invisible decay channels", 2017 [arXiv: 1703.05703]